https://doi.org/10.5194/egusphere-2026-3664
Preprint. Discussion started: 22 July 2026

Hydrological Modeling of Climate Change Impacts on Alpine Catchments: Shifting Snow Dynamics, Runoff Regimes, and the Frequency of Extremes

Simon Seelig[1], Magdalena Seelig[1], Matevž Vremec[1,2], Martin Masten[1], Thomas Wagner[1], Karl Krainer[3], Michael Avian[4], Klaus Haslinger[4], Heike Brielmann[5], Albrecht Leis[6], Markus Ribis[7], Maria Obwegs[1,8], Matthias Hausleber[1,9], Rudolf Philippitsch[10], Richild Mauthner-Weber[10], Ernst Überreiter[10], and Gerfried Winkler[1]

[1]Department of Earth Sciences, NAWI Graz Geocenter, University of Graz, Heinrichstraße 26, 8010 Graz, Austria
[2]Alma Mater Europaea University, Slovenska ulica 17, 2000 Maribor, Slovenia
[3]Institute of Geology, University of Innsbruck, Innrain 52, 6020 Innsbruck, Austria
[4]Department of Climate Impact Research, GeoSphere Austria, Hohe Warte 38, 1190 Vienna, Austria
[5]Team Groundwater, Environment Agency Austria, Spittelauer Lände 5, 1090 Vienna, Austria
[6]JR-AquaConSol, Steyrergasse 21, 8010 Graz, Austria
[7]geo.zt gmbh poscher beratende geologen, Saline 17, 6060 Hall in Tirol, Austria
[8]now at Geo Group Austria ZT GmbH, Reininghausstraße 13a, 8020 Graz, Austria
[9]now at Geoconsult ZT GmbH, Leechgasse 37, 8010 Graz, Austria
[10]Federal Ministry of Agriculture and Forestry, Climate and Environmental Protection, Regions and Water Management, Marxergasse 2, 1030 Vienna, Austria

Correspondence: Simon Seelig (simon.seelig@uni-graz.at)

Abstract. Climate change is fundamentally restructuring the alpine hydrological cycle, yet how shifting snow dynamics interact with aquifer storage to regulate downstream impacts remains poorly constrained. This interaction is particularly critical in mid- to high-altitude headwaters increasingly dominated by rainfall, where sediment accumulations such as rock glaciers act as hydrogeological buffers. To investigate these dynamics, we assess the streamflow response of 15 nested sub-catchments across five study sites in the Austrian Alps, spanning diverse climatic, geomorphic, and geological conditions. High-resolution field observations combined with satellite-derived snow data were used to calibrate a cascading modeling framework that resolves hydrological processes from individual rock glacier springs and small headwaters (<1 km^2) to downstream river catchments up to 200 km^2. Using an ensemble of 40 climate projections across Representative Concentration Pathways (RCP) 2.6, 4.5, and 8.5, we simulate hydrological change through the 21st century. We quantify these impacts in terms of snow and runoff seasonality, magnitude and significance of hydrometeorological index alterations, and shifts in return periods of historical 10-year extremes. Our results indicate a seasonal reorganization of runoff, with the transition from snow-dominated to rain-influenced regimes progressing asynchronously across catchments. This variation in timing is mediated by elevation, morphology, local climate, and bedrock geology, resulting in contrasting responses between headwater and downstream reaches. Headwater catchments are the most vulnerable to these changes, as their localized aquifers are too small to offset declining seasonal snow storage, earlier spring melt, and intensifying summer flow deficit. In contrast, downstream aquifer systems, including karst formations and valley sediments, more effectively dampen these alterations,

https://doi.org/10.5194/egusphere-2026-3664
Preprint. Discussion started: 22 July 2026

although they cannot fully compensate for the loss of cryospheric storage. Across all but the highest elevations, the transition toward rain-dominated regimes drives an asymmetrical shift in hydrological extremes, characterized by more pronounced high flows but less severe low flows. As snow-rich winters decline and the snow season shortens, stronger coupling between precipitation and runoff enhances catchment responsiveness, and more frequent rain-on-snow events amplify early-season peak flows. Conversely, increased winter rainfall and early snowmelt sustain aquifer recharge, thereby buffering streamflow and reducing the severity of low-flow events. Together, these responses show that subsurface storage redistributes changes in flow extremes, yet cannot counteract the broader transition toward a flashier, precipitation-driven runoff regime. This heightened responsiveness of catchment runoff to atmospheric forcing underscores the need for adaptive water management strategies that navigate simultaneous changes in seasonal water budgets, short-term variability, and the shifting frequency of extremes.

1 Introduction

Mountain hydrology is undergoing a systemic transformation driven by altered climate forcing, with consequences cascading from alpine headwaters to main valleys and downstream forelands (Viviroli et al., 2007, 2026; Hock et al., 2019). As the 'water towers' of the world, mountain ranges provide essential ecosystem services by regulating water availability through the storage and release of snow and groundwater (Beniston and Stoffel, 2014; Brighenti et al., 2019b; Immerzeel et al., 2020). However, rising temperatures cause a rapid shift from snow-dominated to rain-dominant regimes, thereby altering the seasonal redistribution of recharge, storage, and runoff across headwaters and downstream catchments (Hanus et al., 2021; Tedesche et al., 2025). This reorganization reduces the reliability of cryospheric storage and forces a greater reliance on the remaining components of the hydrological system, including the diverse sediment accumulations that form alpine aquifers on mountain flanks, in headwater cirques, and in alpine valleys (Hayashi, 2020; Somers and McKenzie, 2020; Arnoux et al., 2021; Siirila-Woodburn et al., 2026). While these large-scale shifts alter storage and release mechanisms globally, the hydrological catchment response differs significantly across altitudinal gradients, ranging from rapid transitions at lower elevations to a more retarded response in high-alpine regions (Staudinger et al., 2015; Blahušiaková et al., 2020). Of particular importance is the transient behavior of mid- to high-altitude catchments, which currently occupy a critical state of hydrological instability as they shift from snow to rain dominance (Speich et al., 2015; Jenicek et al., 2018).

At the mountain-catchment scale, atmospheric warming acts as the primary driver modifying snow dynamics through a complex interplay of competing sensitivities. While climate warming unequivocally reduces overall snow volumes, the resulting impact on snowmelt rates is less straightforward. Higher air temperatures can accelerate melt, yet the potential for sustained melt events is ultimately constrained by the diminishing snowpack (Beniston et al., 2018; Guo et al., 2025). Furthermore, rain-on-snow events are decreasing at lower elevations but increasing at higher altitudes, where a persistent snowpack is now exposed to rainfall (Morán-Tejeda et al., 2016; Musselman et al., 2018; Hotovy et al., 2023, 2025). These dynamics could profoundly reshape the characteristics and propagation of hydrological extremes. First, accelerated snowmelt drives long-lasting, large-scale floods (Berghuijs et al., 2019; Brunner and Fischer, 2022). Second, as the fraction of extreme precipitation falling as snow declines, catchments lose a critical retarding mechanism, which directly amplifies flood peaks

https://doi.org/10.5194/egusphere-2026-3664
Preprint. Discussion started: 22 July 2026

(Hauer et al., 2025; Komma et al., 2025). Conversely, earlier melt coupled with rising evaporative demand induces a progressive upslope shift in low-flow regimes from winter to summer (Laaha et al., 2016; Chartier-Rescan et al., 2025; Masten et al., under review). These transitions represent a fundamental change in alpine water storage, forcing a move from storage-governed seasonal release to an increasingly flashy, rainfall-dominated regime throughout the year (Jenicek et al., 2016, 2018; Hanus et al., 2021). Together, these interactions represent the initial stage of a hydrological cascade, where the changing snow dynamics define the boundary conditions for subsequent downstream propagation.

This downstream impact of climate change is in turn modulated by the internal storage capacity and drainage characteristics of the alpine landscape. While previous research has often focused on the distinct dynamics of glacierized systems, karst aquifers, main valleys, or large-scale foreland basins, most high-elevation headwaters are dominated by a different type of aquifer storage: fragmented, unconsolidated sediment accumulations (Hayashi, 2020; Somers and McKenzie, 2020). Rock glaciers represent a primary example of these features, ranging from ice-rich, actively creeping landforms to relict, largely ice-free features (Berthling, 2011; Jones et al., 2019). They function as porous aquifers in which coarse-grained surface layers typically overlie finer-grained sediments, creating a dual-flow regime that supports both fast preferential pathways and delayed matrix release of water (Winkler et al., 2018; Seelig et al., 2026a). This internal structure provides substantial storage that lags recharge delivery to stream networks by weeks or months, but also allows rapid release of water, contributing to peak flows (Winkler et al., 2016a; Harrington et al., 2018; Wagner et al., 2021a). Despite their documented influence on alpine headwaters (Wagner et al., 2016; Brighenti et al., 2019a, 2026; Bearzot et al., 2023), the specific capacity of these aquifers to mediate shifting runoff patterns along the upstream-downstream continuum remains largely unquantified.

Treating rock glaciers as a diagnostic proxy for shallow porous storage offers a scalable framework to address this limitation. Although part of a broader continuum of sediment accumulations, these landforms serve as diagnostic indicators of catchments characterized by coarse-grained subsurface storage and delayed drainage behavior. Their distribution therefore enables a first-order assessment of how shallow aquifers modulate catchment responses to climatic forcing at local and regional scales. The hydrological relevance of these landforms extends beyond themselves and provides a window into the broader role of alpine subsurface storage in regulating water retention and release. This subsurface buffering capacity is intrinsically coupled with snowmelt dynamics, which govern the seasonal recharge of these porous aquifers.

While previous studies have often examined the effects of changing snow dynamics (e.g., Jenicek et al., 2016, 2018; Meriö et al., 2019) and groundwater processes (e.g., Staudinger et al., 2015; Berghuijs et al., 2016; Paznekas and Hayashi, 2016; Arnoux et al., 2021) independently, few have addressed their combined influence on streamflow variability and runoff response in alpine headwater catchments. This disconnected approach introduces a critical knowledge gap, because projected shifts in snow accumulation and snowmelt timing will propagate through catchments whose runoff behavior is strongly conditioned by internal storage and drainage processes. Tracing these cascading effects downstream necessitates a coupled view of changing surface drivers and internal storage dynamics. Therefore, understanding future water availability and hydrological extremes in mountainous regions requires an integrated perspective that jointly considers climatic forcing and the buffering capacity of alpine aquifers across the upstream–downstream continuum.

https://doi.org/10.5194/egusphere-2026-3664
Preprint. Discussion started: 22 July 2026

This study addresses these uncertainties by investigating the climate sensitivity of 15 nested catchments across five study areas in the Austrian Alps. We employ an ensemble of 40 climate projections partitioned across three emission scenarios (RCP 2.6, 4.5, and 8.5) to quantify how warming trajectories modify snow cover dynamics, seasonal water availability, and hydrological extremes. Our framework integrates high-resolution discharge observations, satellite-derived snow cover data, and hydrological modeling to assess how climatic, geomorphic, and geological factors control the propagation of water from springs to low-order streams. By treating snow cover and subsurface storage as complementary components of the headwater water balance, we evaluate how their joint feedback modulates runoff regimes. This approach aims to provide a process-based assessment of catchment resilience within the evolving alpine hydrological cycle.

2 Study Sites

Five regions were selected across the Austrian Alps to represent hydro-climatic heterogeneity along topographic, climatic, and geological gradients from high-alpine headwaters to mid-altitude basins. These sites enable analysis of how snow dynamics translate into runoff and, owing to their high rock glacier densities (Figure 1, mapped based on Wagner et al., 2020a), how alpine porous aquifers further modulate hydrological responses to climate change.

2.1 Seckau Alps

The easternmost study area, located in the central Seckau Alps (Styria), encompasses the Ingering and Gaal valleys (Figure 1b). Hydrologically defined by the Ingeringbach catchment, the area covers 199 km^2 and spans an elevation range from 749 m a.s.l. at the Hammerjäger gauge to 2417 m a.s.l. at Geierhaupt summit, with a mean elevation of 1522 m a.s.l. (a topographic map is provided in Supplementary Figure S1). The catchment is characterized by 61 relict rock glaciers that drain 14% (27.9 km^2) of the total area (Table 1). Drainage percentages refer to the combined area of the rock glaciers and their contributing catchments (Wagner et al., 2020a).

The pronounced development of these periglacial landforms is attributed to the absence of a continuous ice-stream network during the Last Glacial Maximum (van Husen, 1997). Rapid melting of smaller cirque glaciers led to early permafrost conditions along mountain ridges in the Late Glacial, while extensive till deposits and frost debris provided material for rock glacier formation (Untersweg and Schwendt, 1996).

The climate is the warmest among the five study sites, with a mean annual air temperature of 4.3 °C (1980–2009, based on Hiebl and Frei, 2016). This relatively mild climate restricts modern permafrost to isolated, north-facing summit regions. Mean annual precipitation is 1094 mm, with a potential evapotranspiration of 479 mm (based on Haslinger and Bartsch, 2016; Hiebl and Frei, 2018).

Bedrock is composed of low-permeability metamorphic rocks of the Silvretta–Seckau nappe system, primarily comprising the basement suites of the Seckau Complex (Schmid et al., 2004; Mandl et al., 2022, a geological map is provided in Supplementary Figure S1). The Gaal valley is dominated by gneisses, mica schists, and amphibolites, whereas the Ingering valley additionally contains granites (Pfingstl et al., 2015; Mandl et al., 2018). Due to the low hydraulic conductivity of these

https://doi.org/10.5194/egusphere-2026-3664
Preprint. Discussion started: 22 July 2026

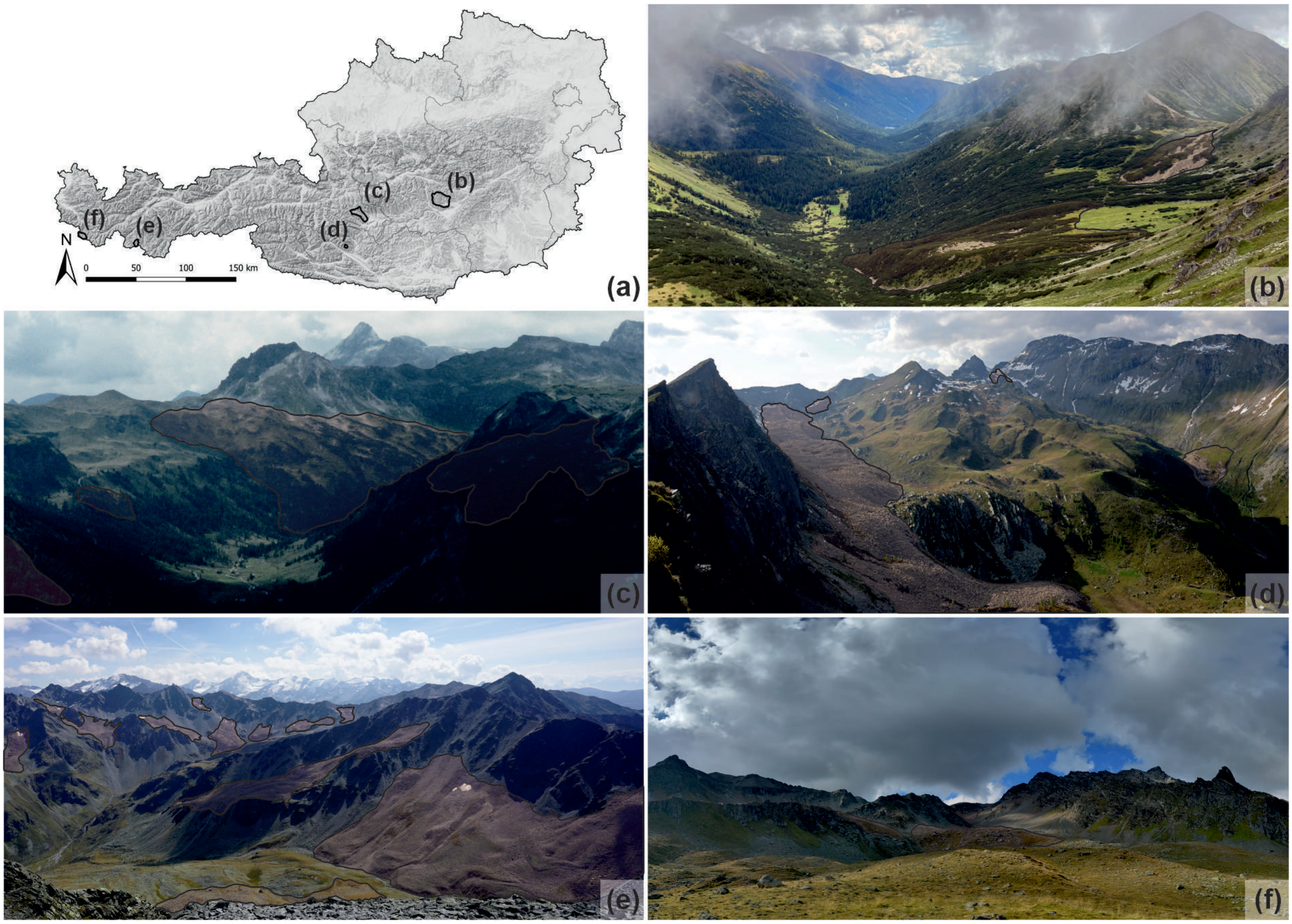

Figure 1. Regional setting and landscape characteristics of the five study areas. (a) Map illustrating the distribution of study sites across the Austrian Alps (relief data: Open Government Data Austria, 2025). (b–f) Representative landscape views of the individual sites, with rock glaciers highlighted in red: (b) Seckau Alps: the Ingering valley headwaters, characterized by prominent relict rock glaciers shaping the mountain flanks (photo: T. Wagner). (c) Radstadt Alps: the upstream catchment area, where rock glaciers occupy the slopes between the valley floor and steep rock faces (photo: S. Seelig). (d) Reißeck Group: the Roßalm area, showing enclosed depressions and a prominent rock glacier bordering southwestern rock walls, with the deeply incised Reinitzbach valley in the background (photo: S. Seelig). (e) Ötztal Alps: the upper study area, dominated by a high density of rock glacier complexes situated beneath steep rock faces (photo: R. Philippitsch). (f) Silvretta Alps: the upstream catchment reaches, showing rock glaciers occupying cirque floors and slopes beneath the main ridges (photo: S. Seelig).

rocks, significant groundwater storage is largely confined to sedimentary deposits: in the headwaters, these are mainly local accumulations such as talus fans and rock glaciers; in the valleys, groundwater is stored in basin- and valley-fill deposits (Metz, 1976; Untersweg and Schwendt, 1996; Winkler et al., 2016a, b).

https://doi.org/10.5194/egusphere-2026-3664
Preprint. Discussion started: 22 July 2026

Table 1. Overview of the five study sites and their nested sub-catchment structure. For each sub-catchment, minimal, mean, and maximum catchment elevation (z_{min}, z_{mean}, z_{max}), area (A), percentage of area draining through rock glaciers (A_{RG}), and the number of ice-containing (RG_I) and relict (RG_R) rock glaciers are reported. Drainage percentages refer to the combined area of the rock glaciers and their contributing catchments (Wagner et al., 2020a).

Study Site	Catchment	z_{min} (m a.s.l.)	z_{mean} (m a.s.l.)	z_{max} (m a.s.l.)	A (km^2)	A_{RG} (%)	RG_I (–)	RG_R (–)
Seckau Alps	Hammerjäger	749	1522	2417	198.93	14	0	61
Seckau Alps	Kettentörlbach	1599	1855	2152	1.48	54	0	4
Seckau Alps	Kettentörlquelle	1609	1870	2124	0.63	99	0	2
Radstadt Alps	Mauterndorf	1108	1801	2687	102.22	18	0	50
Radstadt Alps	Postalm	1295	1934	2687	34.57	31	0	25
Radstadt Alps	Lantschfeldquelle	1734	2060	2375	1.81	98	0	2
Reißeck Group	Ruppalm	1625	2176	2774	7.5	67	1	7
Reißeck Group	Buchleiten	1887	2185	2515	2.25	96	0	4
Reißeck Group	Sonnblick	2170	2309	2515	0.24	0	0	0
Reißeck Group	Ochsenhütte	2022	2355	2774	1.79	15	1	2
Ötztal Alps	Radurschlalpe	1792	2598	3353	24.38	56	46	5
Ötztal Alps	Brunnekarquelle	2363	2605	3000	0.64	81	4	0
Ötztal Alps	Vorderes Bergle	2492	2733	3011	1.24	85	7	0
Ötztal Alps	Arzkarquelle	2542	2843	3218	0.95	100	4	0
Silvretta Alps	Gargellen	1402	2166	2875	39.2	12	14	12
Silvretta Alps	Vergaldaalpe	1791	2283	2875	11.25	12	9	1
Silvretta Alps	Upper Vergaldatal	1958	2376	2875	4.83	27	8	1
Silvretta Alps	Rotbühel	2280	2525	2875	0.75	82	4	0

Two sub-catchments in the Ingering valley headwaters were selected for detailed investigation, both characterized by a significant presence of relict rock glaciers (Supplementary Figure S2, Table 1). The Kettentörlbach catchment (1.48 km^2) contains four rock glaciers covering 54% of its area, whereas the remaining terrain is characterized by rock slopes and alpine meadows. Within this basin, the nested Kettentörlquelle catchment (0.63 km^2) is almost entirely drained by two rock glaciers (99%). Land cover ranges from dense mountain pine in the lower reaches to alpine grasslands and steep rock faces at higher elevations.

2.2 Radstadt Alps

This study area comprises the Lantschfeld and Taurach valleys in the eastern Radstadt Alps (Salzburg), hydrologically corresponding to the Lungauer Taurach catchment at Mauterndorf (1108 m a.s.l.). The 102 km^2 area reaches a maximum elevation of 2687

https://doi.org/10.5194/egusphere-2026-3664
Preprint. Discussion started: 22 July 2026

m a.s.l. at Hochfeind summit, and a mean elevation of 1801 m a.s.l. (Table 1, Supplementary Figure S3). Valley floors are predominantly meadows developed on alluvial fills, while higher elevations are forested or occupied by alpine grasslands, debris fans, moraines, and rock glaciers (Figure 1c). Steep rock walls, often several hundred meters high, define the ridges. During the period 1980–2009, mean annual air temperature was 2.9°C, mean precipitation 1157 mm, and mean potential evapotranspiration 491 mm. Permafrost is restricted to the highest north-facing slopes, with all 50 rock glaciers of the area classified as relict (Wagner et al., 2020a).

The bedrock geology is dominated by low-grade metamorphic carbonate rocks of the Lower Austroalpine Radstadt nappe system, underlain in the west and south by higher-grade metamorphic sedimentary rocks of the Penninic Tauern Window (Supplementary Figure S3; Exner, 1989; Häusler, 1995; Mandl and Matura, 1995; Exner et al., 2005). Thick, often karstified calcareous and dolomitic marbles form prominent aquifers, while phyllites and schists act as local aquitards, directing subsurface flow. Hydrogeology is strongly controlled by the thrust-and-fold architecture of the bedrocks. Regional drainage reflects the interaction of sedimentary deposits (rock glaciers, moraines, debris fans) with bedrock lithology and karstification.

Hydrological analyses adopt a nested-catchment approach to capture scale-dependent variability (Table 1): in the 102 km^2 Mauterndorf catchment, 18% of drainage passes through rock glaciers; in the 35 km^2 Postalm catchment, this rises to 32%; and in the 1.8 km^2 Lantschfeldquelle catchment, 98% are covered by rock glaciers. The relict rock glacier covering large parts of the Lantschfeldquelle catchment is composed of dolomitic marble that rests on phyllites and feeds the main spring.

2.3 Reißeck Group

The study area in the southern Reißeck group (Carinthia) encompasses the Reinitzbach catchment upstream of Ruppalm, with elevations ranging from 1625 to 2774 m a.s.l. (mean 2355 m a.s.l.). The 7.5 km^2 catchment is largely influenced by rock glaciers, which drain 67% (5.0 km^2) of the area (Table 1, Supplementary Figure S4). Seven of the eight rock glaciers are classified as relict, while the highest rock glacier is assumed to contain permafrost ice. For the 1980–2009 period, the mean annual air temperature was 1.0°C, annual precipitation was 1323 mm, and potential evapotranspiration was 514 mm.

Geologically, the area belongs to the Tauern Window and comprises the subpenninic Venediger nappe system (Schmid et al., 2004; Pestal et al., 2006). Summits are dominated by gneisses of the Hochalm core, while bedrock in middle and lower elevations is composed of amphibolites, paragneisses, and mica schists of the Reißeck, Draxel, and Storz complexes (Supplementary Figure S4; Cliff et al., 1971; Exner, 1980, 1984). A prominent NW–SE–striking fault crosses the study area, characterized by intensively fractured rocks that produce high amounts of debris. Together with rock glaciers and moraines, this material forms porous aquifers that feed springs supplying drinking water to the city of Spittal an der Drau (Schuster et al., 2006).

Morphologically, the area comprises three main units (Figure 1d): the topographically complex Roßalm plateau, a deep eastern ravine carved by the Reinitzbach, and cirque- and step-shaped landforms in between. Valley flanks along the Reinitzbach are occupied by extensive unconsolidated sediments of talus slopes, whereas the Roßalm features closed depressions with several small wetlands and perennial standing water bodies (Supplementary Figure S5). A prominent relict rock glacier at the base of steep southwestern escarpments shapes the landscape, occasionally interrupted by transverse bedrock ridges that host

https://doi.org/10.5194/egusphere-2026-3664
Preprint. Discussion started: 22 July 2026

additional ponds. Three sub-basins capture the internal variability of the study area (Table 1): the high-altitude Ochsenhütte (1.79 km^2, 15% rock glacier drainage), the Buchleiten spring on the Roßalm plateau (2.25 km^2, 96% rock glacier drainage), and the smaller, rock-glacier-free Sonnblick catchment (0.24 km^2) nested within the Buchleiten area.

2.4 Ötztal Alps

The Radurschl valley upstream of Radurschlalpe (1792 m a.s.l.) in the western Ötzal Alps (Tyrol) is the highest site among the five study areas and characterized by pronounced alpine conditions. Elevation ranges from 1792 m a.s.l. to a maximum of 3353 m a.s.l. at Glockturm, with a mean elevation of 2598 m a.s.l. The catchment covers 24 km^2, of which 56 % (13 km^2) is drained by rock glaciers (Table 1, Supplementary Figure S6). A total of 51 rock glaciers have been identified, 46 of which are inferred to contain permafrost ice, indicating that permafrost is widespread in the catchment area.

The high elevation results in a long-term mean annual air temperature (1980–2009) of -1.6 °C. Situated within the inner-alpine dry zone, the area receives relatively low mean annual precipitation (974 mm), while potential evapotranspiration is 479 mm. The dry climate and steep morphology favor rock glaciers over glaciers (Kerschner, 1982). During the 20th century, the equilibrium line altitude rose from ∼3100 m a.s.l. to ∼3300 m a.s.l. (Žebre et al., 2021), allowing rock glaciers to dominate the permafrost zone above ∼2400–2600 m a.s.l. (Ribis, 2017). The only glaciers in the catchment, Hüttekarferner and Glockturmferner, cover 0.16 km^2 (0.7% of the area).

Bedrock in the catchment area is composed of ortho- and paragneisses of the Ötztal-Stubai Complex (Supplementary Figure S6; Hoinkes and Thöni, 1993; Tropper and Recheis, 2003; Sölva et al., 2005; Moser, 2012), which is part of the Ötztal–Bundschuh nappe system (Schmid et al., 2004). The upper study area is dominated by steep rock walls, talus slopes, rock glaciers, and till deposits, forming extensive coarse-grained sediment deposits that mantle large portions of the cirques and gentler slopes (Figure 1); vegetation is sparse and discontinuous, with only patchy alpine grassland developed on thin, poorly evolved soils. In contrast, the lower parts are characterized by alpine meadows and forests, where soils are more developed and continuous.

Three high-alpine headwater catchments were analyzed (Table 1). Their headwaters are located in the uppermost parts of the study area, which are dominated by coarse-grained sediment deposits. Arzkar (0.95 km^2) forms a small cirque beneath the summit of Glockturm and is drained almost entirely (99.5%) by four rock glaciers assumed to contain permafrost ice. Brunnekar (0.64 km^2) comprises four rock glaciers with ice situated on the eastern flank of Wildnörderer, which drain 81% of the catchment. Vorderes Bergle (1.24 km^2), extends between the summits of Wildnörderer and Nördlicher Seekarkopf and hosts seven ice-containing rock glaciers, which drain 85% of the catchment.

2.5 Silvretta Alps

The westernmost study area encompasses 39 km^2 in the Vergalda and Valzifenz valleys of the western Silvretta Alps (Vorarlberg). Hydrologically, it is represented by the Suggadinbach catchment at Gargellen (1402 m a.s.l.), extending to an elevation of 2875 m a.s.l. at the Eisentälispitze summit, with a mean elevation of 2166 m a.s.l. (Table 1, Figure 1f). The upper reaches are influenced by permafrost, with 14 of 26 rock glaciers assumed to contain permafrost ice (Supplementary Figures S7 and S8).

https://doi.org/10.5194/egusphere-2026-3664
Preprint. Discussion started: 22 July 2026

During the period 1980–2009, the mean annual air temperature was 0.7 °C, mean annual precipitation was 1571 mm, and mean annual potential evapotranspiration amounted to 537 mm.

The central and eastern sectors of the catchment are dominated by gneiss and amphibolite of the Silvretta Nappe (Silvretta–Seckau Nappe System, Supplementary Figure S7; Oberhauser and Rataj, 1998; Schmid et al., 2004). In the western parts, Penninic units are exposed in a tectonic window (Gargellen Window) that is composed of sedimentary rocks of four tectonically thinned nappes (Prättigauflysch, Falknis Nappe, Sulzfluh Nappe, and Arosa Zone). Hydrogeologically, the most significant units are the up to 70 m thick, highly karstified limestones of the Sulzfluh Nappe, which are largely overlain by the low-permeability metamorphic rocks of the Silvretta Nappe. The Suggadinbach cuts through these limestones, forming a significant spring horizon, which suggests that part of its discharge may originate outside the orographic catchment along its western boundary (Mathis, 2005).

Drainage dynamics were analyzed using a nested hierarchy in the Vergalda valley, which captures the decreasing hydrological influence of rock glaciers along the flow path (Table 1): from the spring at Rotbühel (0.75 km^2; 82% rock glacier drainage) through Upper Vergaldatal (4.83 km^2; 27%) to the Vergaldaalpe catchment (11.25 km^2; 12%). Three water diversions (Vergaldabach, Valzifenzbach, and Madrisa Springs) transfer water to the Vermunt Reservoir; their locations and associated catchments are shown in Supplementary Figure S9. The volumes diverted are continuously monitored and explicitly included in the water balance and model setup.

3 Methods

3.1 Hydrometeorological Data and Climate Scenarios

Meteorological forcing data were obtained from gridded products provided by GeoSphere Austria. To ensure long-term homogeneity, these datasets rely on selected weather stations and interpolation schemes that explicitly account for mountainous topography. For reproducing historical records with model simulations, we utilized the Spatiotemporal Reanalysis Dataset for Climate in Austria (SPARTACUS), which provides daily precipitation and air temperature at 1 × 1 km resolution (Hiebl and Frei, 2016, 2018). Potential evapotranspiration was extracted from the Austrian Reference Evapotranspiration dataset (ARET), a derivative of SPARTACUS that incorporates minimum/maximum temperatures and extraterrestrial radiation (Haslinger and Bartsch, 2016). We utilized a recently updated ARET energy balance representation, which incorporates long-wave radiation through correction fields (Haslinger et al., 2023). Meteorological variables were averaged across each catchment using areal weighting of the grid cells.

Observational targets for model calibration were established through a dedicated field monitoring program and satellite-derived data. We installed 14 gauging stations (Dipper-PTEC, SEBA Hydrometrie) to record water level at 30-minute intervals from 2020 to 2022. Stage–discharge relationships were established using 207 discharge measurements across varying water levels. At three locations (Sonnblick, Brunnekar, Upper Vergaldatal), the gauging stations were destroyed during the winter months, and despite repairing them in spring we could not establish a reliable rating curve, thus these were discarded from the analysis. At four locations, data collected during the high-alpine monitoring campaign were complemented by long-term

https://doi.org/10.5194/egusphere-2026-3664
Preprint. Discussion started: 22 July 2026

discharge series from second-order rivers spanning 28 to 61 years (Hammerjäger, Mauterndorf, Radurschlalpe, Gargellen). Additionally, we estimated daily snow-covered area for five elevation bands using MODIS C6.1 data (500 × 500 m resolution). Based on the Normalized Difference Snow Index (NDSI), we captured the snow cover fraction per pixel from 2002–2022, leveraging the improved accuracy of the C6.1 version for mountainous terrain (Riggs et al., 2019).

Future climate projections were integrated via the ÖKS15 dataset. This framework provides daily maximum/minimum temperatures, precipitation, and global radiation for three emission scenarios reflecting diverse socio-economic development pathways (RCP 2.6, 4.5, and 8.5, Chimani et al., 2020). This setup was used to capture spatial variability associated with complex topography and elevational gradients in alpine catchments. It includes a selected ensemble of climate models from the EURO-CORDEX EUR-11 archive, comprising 8 runs for RCP2.6 alongside 16 runs each for RCP4.5 and RCP8.5. These models were bias-corrected using a trend-preserving method and downscaled to a 1 × 1 km grid (Jacob et al., 2014; Switanek et al., 2017).

3.2 Hydrological Modeling Framework

The hydrological catchment response was simulated using a parsimonious lumped-parameter model implemented in the airGR environment (Coron et al., 2017). The modeling chain, depicted schematically in Supplementary Figure S10, couples the semi-distributed snow model CemaNeige (Valéry et al., 2014b) with the rainfall-runoff model GR4J (Perrin et al., 2003). This framework was chosen for its conceptual efficiency in water flux simulation, having been validated across extensive comparative studies for both, river and spring flow simulations (Moussu, 2011; Valéry, 2010; Valéry et al., 2014a; Wagner et al., 2016, 2021b; Lavenne et al., 2019; Riboust et al., 2019; Sezen et al., 2019; Citrini et al., 2020; Ollivier et al., 2020; Bertolotti et al., 2026; Masten et al., 2026).

In each study area, at least one rock glacier spring was monitored to constrain the local hydrogeological functioning of rock glacier systems. Following a parameter regionalization approach based on catchment similarity (Blöschl et al., 2013), the model parameters were first calibrated against these spring discharge records and subsequently transferred to all other rock glaciers and their associated catchments within the same study area. This approach assumes that rock glaciers act as the dominant rate-controlling hydrogeomorphical units within their headwater catchments (Hayashi, 2020; Wagner et al., 2020b). Downstream catchments were then modeled by propagating upstream simulations through a lag-and-route model (Bentura and Michel, 1997; Lavenne et al., 2019) and accounting for additional local inputs, thereby preserving process coherence across nested spatial scales.

Snow cover and melt dynamics were modeled using the CemaNeige snow routine (Valéry et al., 2014a, b), applied separately to five equal-area elevation bands derived from a 10-meter digital elevation model (Open Government Data Austria, 2025). The model discriminates precipitation into rain and snow based on air temperature, with a transition phase between -1 °C and +3 °C. Snowmelt is calculated using an enhanced degree-day approach that accounts for the snowpack's cold content, the heat required to warm it to 0 °C. The model parameters θ_1 (degree-day factor) and θ_2 (cold-content factor) control melt rates and the responsiveness of the snowpack energy deficit to temperature variations. Our model setup addresses the characteristic heterogeneity of alpine snowpacks by introducing a linear hysteresis between snow-covered area (*SCA*) and snow water

https://doi.org/10.5194/egusphere-2026-3664
Preprint. Discussion started: 22 July 2026

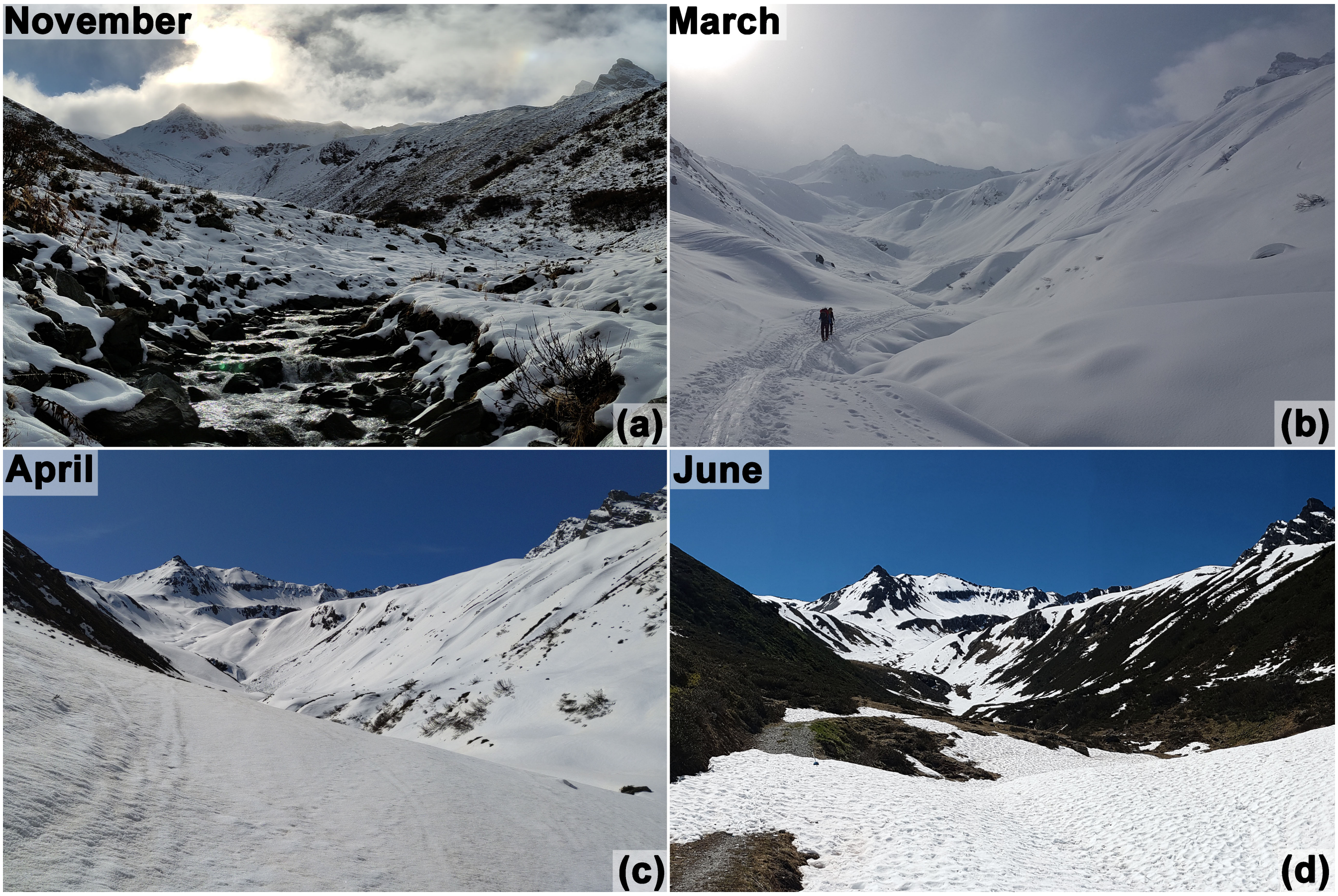

Figure 2. Snow cover development in the Silvretta Alps during the study period. The relationship between snow-covered area and snow mass exhibits significant hysteresis, driven by varying melt and accumulation patterns across complex terrain. (a) Early winter accumulation: fresh snow rapidly blankets the terrain, producing a thin, widespread snow cover (snow-covered area (*SCA*) high, snow water equivalent (*SWE*) low). (b) Late winter: thick snow covers nearly the entire catchment, with only steep rock walls remaining snow-free (*SCA* high, *SWE* high). (c) Early spring: ridges and slopes exposed to the sun melt quickly, while dense snow persists in depressions and shaded areas (*SCA* moderate, *SWE* high). (d) Late spring: snow remains only in shadowed terrain and depressions (*SCA* low, *SWE* low). Comparable dynamics across all study sites highlight the importance of explicitly accounting for snow cover hysteresis in the model (Riboust et al., 2019; Masten et al., 2026). Photos: S. Seelig.

equivalent (*SWE*), parameterized by θ_3 and θ_4. This rationale reflects the differing evolution of snow during accumulation (where fresh snow quickly blankets the terrain) and ablation (where ridges become snow-free while dense patches persist in depressions) in mountainous terrain, in line with field observations at the study sites (Figure 2). This parameterization of the snow cover hysteresis has proven particularly stable for alpine catchments, improving long-term model robustness under changing climate conditions (Riboust et al., 2019; Masten et al., 2026).

https://doi.org/10.5194/egusphere-2026-3664
Preprint. Discussion started: 22 July 2026

Catchment-scale runoff generation and routing were simulated using the parsimonious GR4J model (Perrin et al., 2003). In this framework, water enters a soil moisture accounting store with storage capacity x_1, where it is either released via evapotranspiration or infiltrates gradually into the deeper subsurface. As the store becomes more saturated, a progressively larger fraction of the incoming water bypasses it instead. From there, the model conceptually differentiates two flow paths: a fast-flow component transferred via unit hydrograph routing, and a slow-flow component that fills a routing store with capacity x_3 accounting for groundwater storage within alpine aquifers. Flow dynamics are controlled by model parameters x_2, which describes net inter-catchment exchange fluxes not captured by observations, and x_4, which determines the time base of the unit hydrograph. Downstream routing and spatial coherence were maintained through a cascading semi-distributed configuration using a lag-and-route model with celerity c (Bentura and Michel, 1997; Lavenne et al., 2019). This linkage addresses temporal delays caused by channel roughness, flow path lengths, and the attenuation effects of mountain lakes.

In a first step, model optimization utilized a multi-objective strategy based on the modified Kling-Gupta Efficiency (KGE') to match simulations and historical records. This criterion allows for the independent evaluation of correlation, bias, and variability. The primary calibration target was the recorded spring or river discharge (75% weight), supplemented by the MODIS-derived snow cover averaged across each elevation band ($5 \times 5\%$ weight). To infer parameter plausibility, our results were benchmarked against established distributions from 420 catchments for GR4J, 380 for CemaNeige, and 1,300 for the lag-and-route component (Perrin et al., 2003; Lerat et al., 2012; Lobligeois et al., 2014; Valéry et al., 2014a, b; Lavenne et al., 2019; Riboust et al., 2019), while also being evaluated against local catchment characteristics (detailed in Appendix A). In a second step, the calibrated models were forced with climate projections to simulate runoff under various RCP scenarios, allowing assessment of potential hydrological responses to changing climate conditions.

3.3 Hydrometeorological indices and extreme value analysis

To quantify climate change impacts on hydrological regimes, we calculated a suite of metrics characterizing changes in discharge magnitude, seasonality, and extremes, as well as associated meteorological and cryospheric controls. Climate change signals were defined as absolute differences between future and reference conditions for spring or river discharge and snow cover *SWE* within each catchment (following Haslinger et al., 2023). Analyses were conducted for three 30-year periods: a historical baseline (1980–2009), a near-future horizon (2030–2059), and a far-future horizon (2070–2099). Climate change signals were calculated on monthly and annual scales and normalized by catchment area.

In addition, a comprehensive suite of hydrometeorological indices is used to extract key characteristics from the simulation outputs (Table 2). We selected indices shown to reflect hydro-climatic shifts in both alpine springs (Vremec et al., 2025) and river systems (Bard et al., 2015; Jenicek et al., 2016, 2018). By comparing these indices among the three reference periods, we aim to identify not only differences in average conditions, but also systematic shifts in the timing and distribution of hydrological events. Seasonal indices are computed for winter (DJF), spring (MAM), summer (JJA), and autumn (SON), while annual indices are defined over the hydrological year (November 1–October 31).

Within this framework, the first subset of indices isolates the magnitude and temporal variability of discharge. Mean annual discharge (Q) captures the overall water availability, while seasonal means (Q_{DJF}, Q_{MAM}, Q_{JJA}, Q_{SON}) allow the assessment

https://doi.org/10.5194/egusphere-2026-3664
Preprint. Discussion started: 22 July 2026

Table 2. Summary of hydrometeorological indices used in this study. The indices characterize discharge, meteorological forcing, and cryospheric conditions across annual and seasonal scales. Seasonal values are reported for winter (DJF: December–February), spring (MAM: March–May), summer (JJA: June–August), and autumn (SON: September–November). Discharge and climate variables are aggregated over the same seasonal windows. Annual indices are defined over the hydrological year (November 1–October 31). Snow-related metrics are derived from modeled snow water equivalent (*SWE*) and snowmelt time series. DOY denotes day of the year.

Attribute	Description	Unit
Q	Mean annual and seasonal (DJF, MAM, JJA, SON) discharge	mm
P_{max}	Maximum Pardé coefficient	–
RB	Richards-Baker index	–
Q_{7min}	7-day minimum flow (low-flow) discharge	mm
D_{7min}	Timing of 7-day minimum flow (low-flow) discharge	DOY
Q_{max}	Maximum (high-flow) discharge	mm
D_{max}	Timing of maximum (high-flow) discharge	DOY
P	Mean annual and seasonal (DJF, MAM, JJA, SON) precipitation	mm
AT	Mean annual and seasonal (DJF, MAM, JJA, SON) air temperature	°C
ET	Mean annual and seasonal (DJF, MAM, JJA, SON) actual evapotranspiration	mm
P_s	Snow fraction of precipitation (solid precipitation divided by total precipitation)	–
PDD	Positive degree days (> 0°C)	°C
S_{max}	Maximum snow cover *SWE*	mm
D_{Smax}	Timing of maximum snow cover *SWE*	DOY
S_{dur}	Snow cover duration (number of days with *SWE* > 1 mm)	days
M	Total annual snowmelt	mm
M_{max}	Maximum daily snowmelt	mm
D_{Mmax}	Timing of maximum daily snowmelt	DOY

of potential shifts in runoff distribution. The maximum Pardé coefficient (P_{max}) was used as a measure of runoff seasonality throughout the hydrological year, while the Richards-Baker flashiness index (RB) was calculated to quantify the frequency and rapidity of short-term fluctuations in discharge relative to total flow (Baker et al., 2004; Blöschl et al., 2013; McMillan, 2020). To quantify changes in extreme flow magnitude and timing, we derived the annual maximum high-flows (Q_{max}) and 7-day minimum low-flows (Q_{7min}), along with the corresponding day-of-year (DOY) for these events (D_{max} and D_{7min}) (Blöschl et al., 2017; Laaha et al., 2016, 2017).

To better understand the drivers of hydrological changes, we complemented these discharge-related indices with a set of meteorological and cryospheric indicators. Atmospheric drivers were evaluated using total and seasonal precipitation (P), air temperature (AT), and actual evapotranspiration (ET). To quantify snow dynamics, we included the snow fraction of precipitation (P_s), positive degree days (PDD), and several indices characterizing snow cover evolution: maximum *SWE* (S_{max})

https://doi.org/10.5194/egusphere-2026-3664
Preprint. Discussion started: 22 July 2026

and its timing (D_{Smax}), snow cover duration (S_{dur}), total annual snowmelt (M), and peak snowmelt (M_{max}) along with its corresponding timing (D_{Mmax}) (Hock, 2003; Berghuijs et al., 2014; Klein et al., 2016).

We compared these indices across the three 30-year periods for each catchment and RCP. Statistical significance of projected changes between the reference and future periods was evaluated using the non-parametric rank-sum test to distinguish systemic climate signals from internal model variability, with results reported at a significance level of $\alpha = 0.05$ (Wilcoxon, 1945; Helsel et al., 2020). The magnitude of differences was quantified using Hodges–Lehmann (HL) estimates (Hodges and Lehmann, 1963; Hollander et al., 2014), with p-values reported for all comparisons. Seasonal shifts were examined by comparing the timing of extreme flows, peak snow accumulation, and melt events across periods. This provides an understanding of whether observed changes reflect gradual trends or are characterized by a redistribution of water availability across the seasons, such as shifts from winter-dominated to summer-dominated low-flow conditions. By applying this statistical procedure across all time periods, emission scenarios, and indicators, we evaluate climatic, hydrological, and cryospheric shifts within a single, consistent inference framework. The resulting synthesis of these metrics provides a 'hydrological fingerprint' of climate change across the diverse study sites.

Changes in the probability of rare snow and runoff events were quantified through extreme value analysis. To assess changes in event frequency, a threshold-based approach was adopted (Haslinger et al., 2023): a 10-year return level from the historical period served as a reference event. This threshold was then evaluated against fitted distributions of future simulations to estimate its corresponding return period under projected conditions. From this, a frequency amplification factor was derived, quantifying how often historically rare events are expected to occur in the future across catchments and emission scenarios. Return periods were defined as the inverse of occurrence probability, based on annual series. We analyzed maximum snow water equivalent (SWE), maximum snowmelt, and high flows using exceedance probabilities, while 7-day low flows were characterized using non-exceedance probabilities to capture lower-tail behavior (Khaliq et al., 2006). Theoretical distributions were fitted to the data using L-moments, with the generalized extreme value (GEV) distribution applied to SWE, snowmelt, and high flows, and a three-parameter Weibull distribution used for low flows (Chin, 2013; Laaha et al., 2017).

4 Results and Discussion

Our analysis of alpine catchment response to climate forcing shows that changes in snow cover strongly alter seasonal variations in discharge and hydrological extremes downstream, with aquifer systems modulating this response through spatially heterogeneous storage systems. To quantify these changes, we first assessed model performance in the historical period, then examined how declining snowpack storage will translate into future flow regimes, and finally evaluated the corresponding redistribution of hydrological extremes.

4.1 Model Performance and Parameter Plausibility

Hydrological modeling closely matched observed flows and maintained internal consistency across the nested catchment structure. Model performance was high for all 15 catchments, with KGE′ values ranging from 0.74 to 0.93. The models

https://doi.org/10.5194/egusphere-2026-3664
Preprint. Discussion started: 22 July 2026

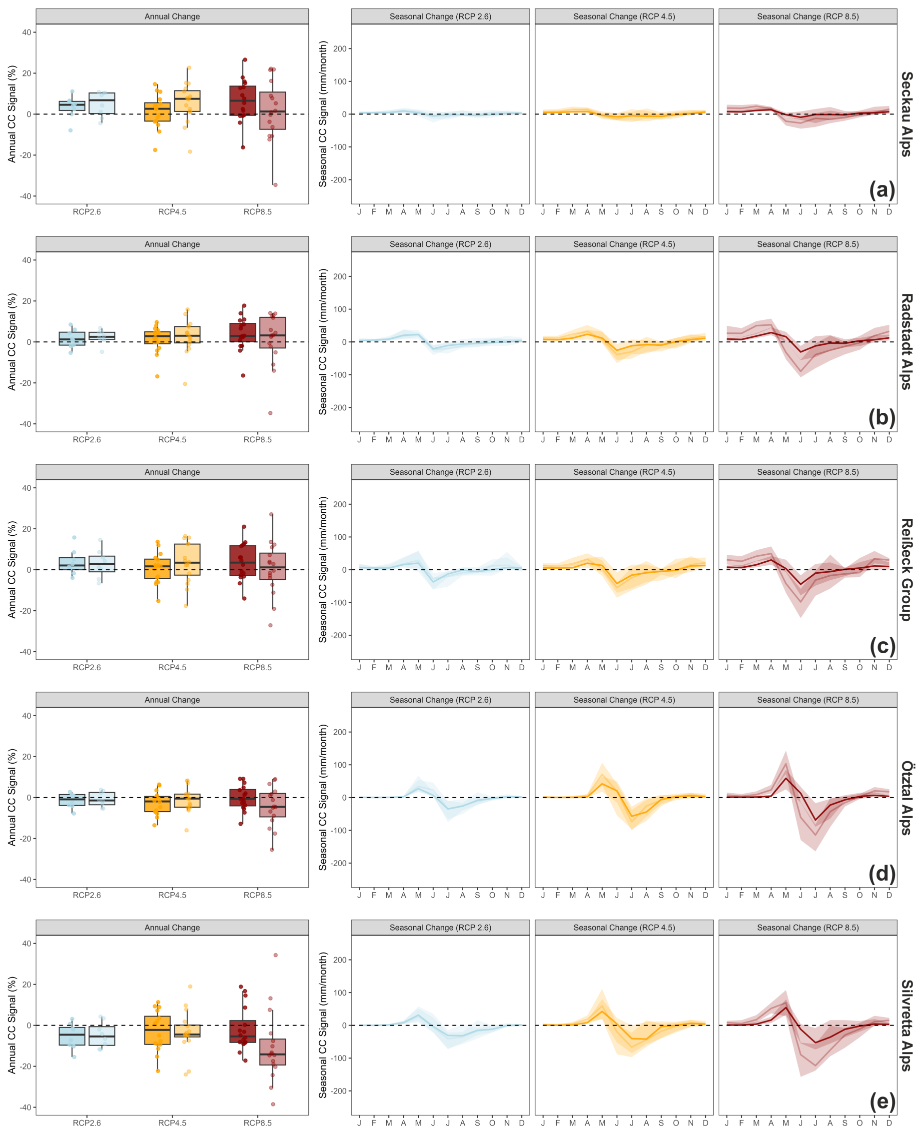

Figure 3. Climate change (CC) signals in discharge at five study sites: (a) Seckau Alps, (b) Radstadt Alps, (c) Reißeck Group, (d) Ötztal Alps, and (e) Silvretta Alps. Changes are shown relative to the historical reference period (1980–2009) for the near-future (2030–2059; saturated colors) and far-future (2070–2099; faded colors) horizons, by emission scenario: RCP2.6 (blue), RCP4.5 (orange), RCP8.5 (red). Boxplots indicate annual discharge changes (relative, left panels), while seasonal changes (mm/month, right panels) show ensemble medians as lines and projection uncertainty as shaded areas. Full runoff projections for individual catchments are provided in Supplementary Figures S26–S30.

reproduced key hydrograph characteristics with high accuracy, capturing both timing and variability, as indicated by strong

https://doi.org/10.5194/egusphere-2026-3664
Preprint. Discussion started: 22 July 2026

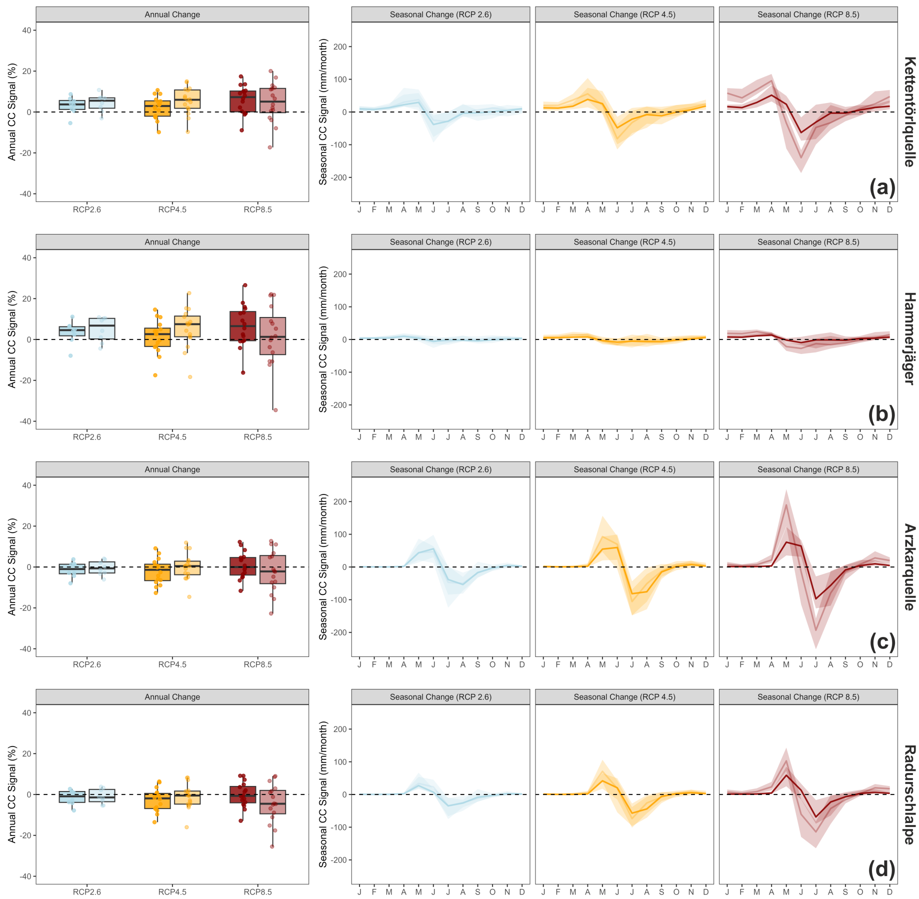

Figure 4. Comparison of climate change (CC) signals in discharge between upstream spring catchments and downstream rivers at two study sites, the Seckau Alps and Ötztal Alps: (a) Kettentörlquelle, a rock glacier spring in the Seckau Alps; (b) downstream Ingeringbach at Hammerjäger, Seckau Alps; (c) Arzkarquelle, a rock glacier spring in the Ötztal Alps; (d) downstream Radurschlbach at Radurschlalpe, Ötztal Alps. Changes are shown relative to the historical reference period (1980–2009) for the near-future (2030–2059; saturated colors) and far-future (2070–2099; faded colors) horizons, disaggregated by emission scenario: RCP2.6 (blue), RCP4.5 (orange), RCP8.5 (red). Boxplots depict ensemble-based changes in annual discharge (relative, left panels), while seasonal changes (mm/month, right panels) show ensemble medians as lines and projection uncertainty across the climate model ensemble as shaded areas.

correlation, low bias, and consistent variance between simulated and observed discharge and snow cover (Appendix A, Supplementary Figures S11–S25).

Beyond performance metrics, the calibrated parameter sets were hydrologically plausible and consistent with physical catchment characteristics. Parameter values reflected contrasts between steep, sparsely vegetated headwaters and downstream valley systems with developed soils, as well as the influence of rock glaciers, wetlands, and karstified bedrock on storage and flow processes. The spatial coherence of parameters across nested catchments, together with their agreement with ranges

https://doi.org/10.5194/egusphere-2026-3664
Preprint. Discussion started: 22 July 2026

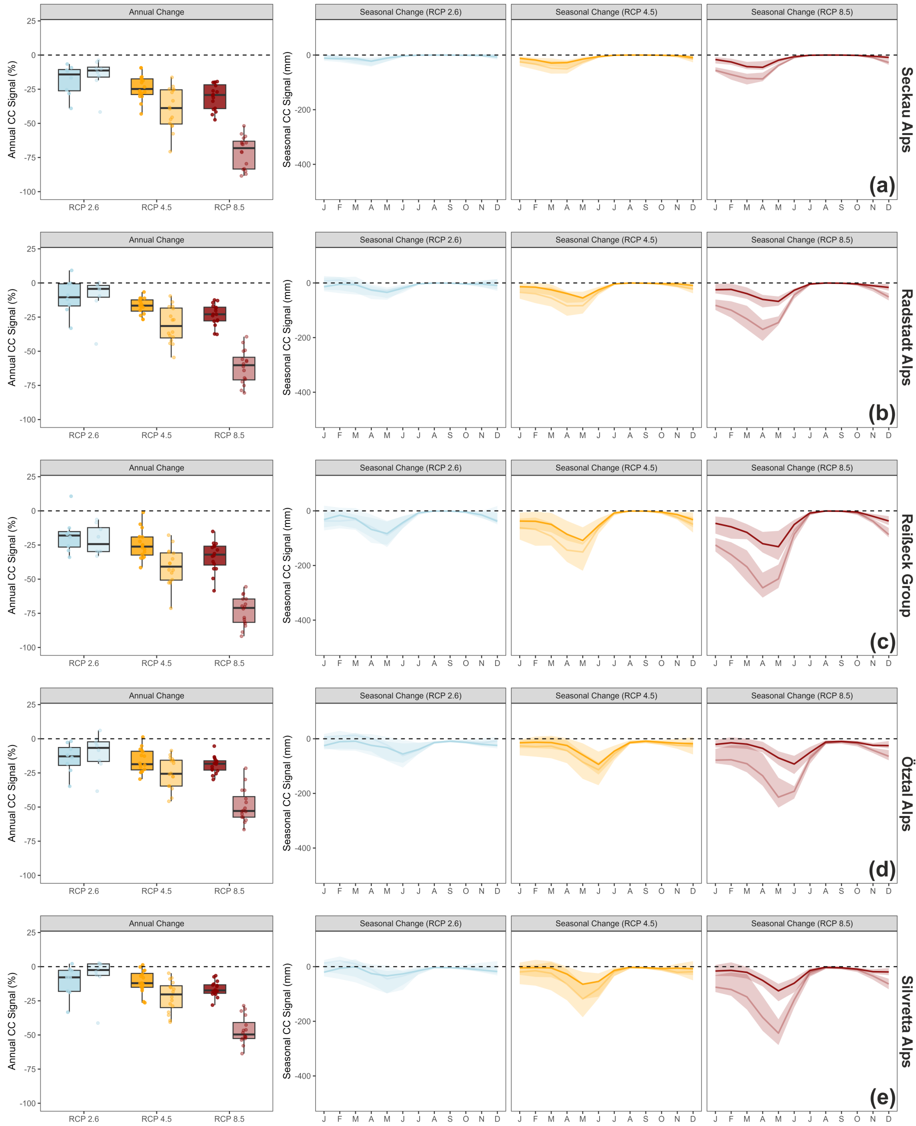

Figure 5. Climate change (CC) signals in average snow cover *SWE* at five study sites: (a) Seckau Alps, (b) Radstadt Alps, (c) Reißeck Group, (d) Ötztal Alps, and (e) Silvretta Alps. Changes are shown relative to the historical reference period (1980–2009) for the near-future (2030–2059; saturated colors) and far-future (2070–2099; faded colors) horizons, by emission scenario (RCP2.6, RCP4.5, RCP8.5). Boxplots indicate annual *SWE* changes (relative, left panels), while seasonal changes (mm, right panels) show ensemble medians as lines and projection uncertainty as shaded areas. Full snow cover *SWE* projections are provided in Supplementary Figures S31–S35.

documented in the literature, supported the physical realism of the model setup. A comprehensive evaluation of model performance, parameter plausibility, and site-specific characteristics is provided in Appendix A.

https://doi.org/10.5194/egusphere-2026-3664
Preprint. Discussion started: 22 July 2026

4.2 Spatial Patterns of Hydrological Change

Driving the calibrated models with climate scenarios reveals moderate changes in future annual runoff, but substantial alterations in seasonal dynamics, with responses differing by emission scenario and catchment characteristics.

Most projections indicate a slight increase in mean annual discharge for the Seckau Alps, Radstadt Alps, and Reißeck Group, whereas more westerly catchments in the Ötztal and Silvretta Alps tend toward a moderate decline (Figure 3). This pattern aligns with the projected east–west gradient in atmospheric water balance (Haslinger et al., 2023): in the western Central Alps, precipitation is expected to change only marginally, while rising evaporative demand leads to a net decrease in water availability. In the eastern regions, increases in precipitation outweigh the enhanced evaporative demand, resulting in a positive atmospheric water balance change. When averaged over 30-year periods, annual catchment runoff largely reflects these long-term atmospheric water balance trends, as short-term snow and subsurface storage fluctuations with characteristic timescales of ∼weeks–months tend to cancel out over time.

In contrast, a pronounced and coherent seasonal climate change signal emerges across all regions: increased discharge in spring due to earlier snowmelt, followed by reduced summer flows as evapotranspiration increases and subsurface storage is depleted earlier (Figure 3; Supplementary Figures S26–S30 show results for individual catchments). The timing of these shifts depends on elevation, occurring earlier in mid-altitude catchments (spring surplus: March–May; summer deficit: June–July) and later in high-alpine systems (surplus: April–June; deficit: July–September). Autumn changes remain small across all catchments, whereas winter runoff increases overall, most strongly in lower-elevation catchments. Seasonal shifts are particularly pronounced under high-emission scenarios and in the late century.

These patterns are modulated by catchment storage, which becomes apparent when comparing upstream and downstream systems: in the Seckau Alps, for example, both the headwater Kettentörlquelle (Figure 4a) and the downstream Hammerjäger catchment (Figure 4b) show increasing annual discharge, but the seasonal signal is strongly dampened downstream due to extensive valley-bottom aquifers that temporarily store water, thereby buffering changes in recharge seasonality. In contrast, the headwater system at Kettentörlquelle responds more directly, as rock glacier storage provides limited attenuation. A similar but more pronounced response is observed in the Ötztal Alps, where the headwater spring Arzkarquelle undergoes strong seasonal shifts (Figure 4c), while downstream river at Radurschlalpe shows seasonal patterns in attenuated form due to larger subsurface storage (Figure 4d). The study sites in the Radstadt Alps, the Reißeck Group, and the Silvretta Alps follow this overall pattern of dampened response in downstream catchments with substantial storage in karst aquifers and thick valley-fill deposits (Supplementary Figures S27, S28, S30). These contrasts highlight how aquifer type and storage capacity control the attenuation of climate-change impacts along the upstream–downstream continuum.

The projected runoff changes are closely linked to altered snowpack dynamics, which provide the underlying control on the seasonal redistribution of water. Figure 5 illustrates the evolution of average snow water equivalent (*SWE*) across the five study regions (Supplementary Figures S31–S35 show individual catchment results). Overall, the simulations indicate a near-universal decline in snow storage, with the strongest reductions occurring during late spring or early summer, consistent with the earlier timing of downstream runoff. The seasonality and magnitude of these declines vary systematically with elevation.

https://doi.org/10.5194/egusphere-2026-3664
Preprint. Discussion started: 22 July 2026

In mid-altitude regions, the largest reductions occur in April–May (Figure 5a,b), whereas in high-alpine regions, the largest reductions shift to May–June (Figure 5d,e). These declines intensify under higher emission scenarios and in the far future, with a tendency toward earlier occurrence of peak reductions. Both the elevation-dependent shifts and the overall strong decline in *SWE* are consistent with findings from similar elevation ranges in the region (e.g., Laghari et al., 2011; Marty et al., 2017). Overall, the projected reduction and shift in snow storage complement earlier spring flow peaks and summer deficits, becoming increasingly decoupled further downstream due to catchment storage and flow routing.

4.3 Hydrometeorological Indices of Change

To characterize the dynamic evolution of snow cover and catchment runoff, we analyze shifts in hydrometeorological indices focusing on their spatiotemporal patterns. Figure 6 shows the ensemble spread of indices characterizing seasonal runoff by study site, period, and RCP scenario. Significant changes relative to the historical reference period (at the $\alpha = 0.05$ level) are indicated by an asterisk below the respective boxplots. The magnitude (HL) and *p*-values of these changes are quantified in Supplementary Table S1.

The results show consistent shifts in discharge across all catchments. Annual changes are small yet often statistically significant (Figure 6a), with increases in the eastern catchments (Seckau Alps, Radstadt Alps, Reißeck Group) and decreases in the western catchments (Ötztal and Silvretta Alps). Comparing these trends with precipitation and evapotranspiration corroborates the previously described east–west gradient of atmospheric water balance: evapotranspiration (*ET*) increases significantly across all catchments, while precipitation (*P*) shows a strong increase in the eastern regions and a more moderate increase in the west (Supplementary Figure S36a,b).

However, the most pervasive signals arise from a seasonal redistribution of discharge: winter discharge (Q_{DJF}) increases significantly (Figure 6b), especially at mid-altitude catchments (Seckau Alps, Radstadt Alps, Reißeck Group), while spring discharge (Q_{MAM}) increases strongly across all catchments (Figure 6c). In contrast, summer discharge (Q_{JJA}) decreases consistently and significantly (Figure 6d). Autumn discharge (Q_{SON}) shows no robust large-scale trend, although individual catchments and emission scenarios exhibit moderate changes in either direction (Figure 6e). The overall discharge seasonality (P_{max}) tends to decrease, especially in the mid-altitude regions; at the higher-elevation sites in the Ötztal and Silvretta Alps, these shifts become significant later in the century and even then only for the high-emission scenarios (Figure 6f).

Quantifying these changes using HL estimates reveals pronounced differences in magnitude across seasons (Supplementary Table S1). Annual discharge changes vary between +66 mm and -138 mm, while seasonal shifts include increases in winter and spring flows by up to +108 mm and +155 mm, respectively. Conversely, summer flows exhibit a substantial decrease of up to -229 mm. The extent of these shifts is not systematically related to the percentage of catchment area draining through rock glaciers, indicating that they lack sufficient storage capacity to buffer the loss of cryospheric storage (Supplementary Figure S37). In contrast, downstream catchments with extensive karst aquifers or valley-fill sediments—such as Hammerjäger (Seckau Alps), Mauterndorf (Radstadt Alps), and Gargellen (Silvretta Alps)—consistently exhibit a greater capacity to dampen these seasonal shifts, showing distinctly attenuated changes (Supplementary Figure S37). Overall, these results indicate a pronounced shift toward earlier runoff generation, primarily driven by amplified winter and spring flows.

https://doi.org/10.5194/egusphere-2026-3664
Preprint. Discussion started: 22 July 2026

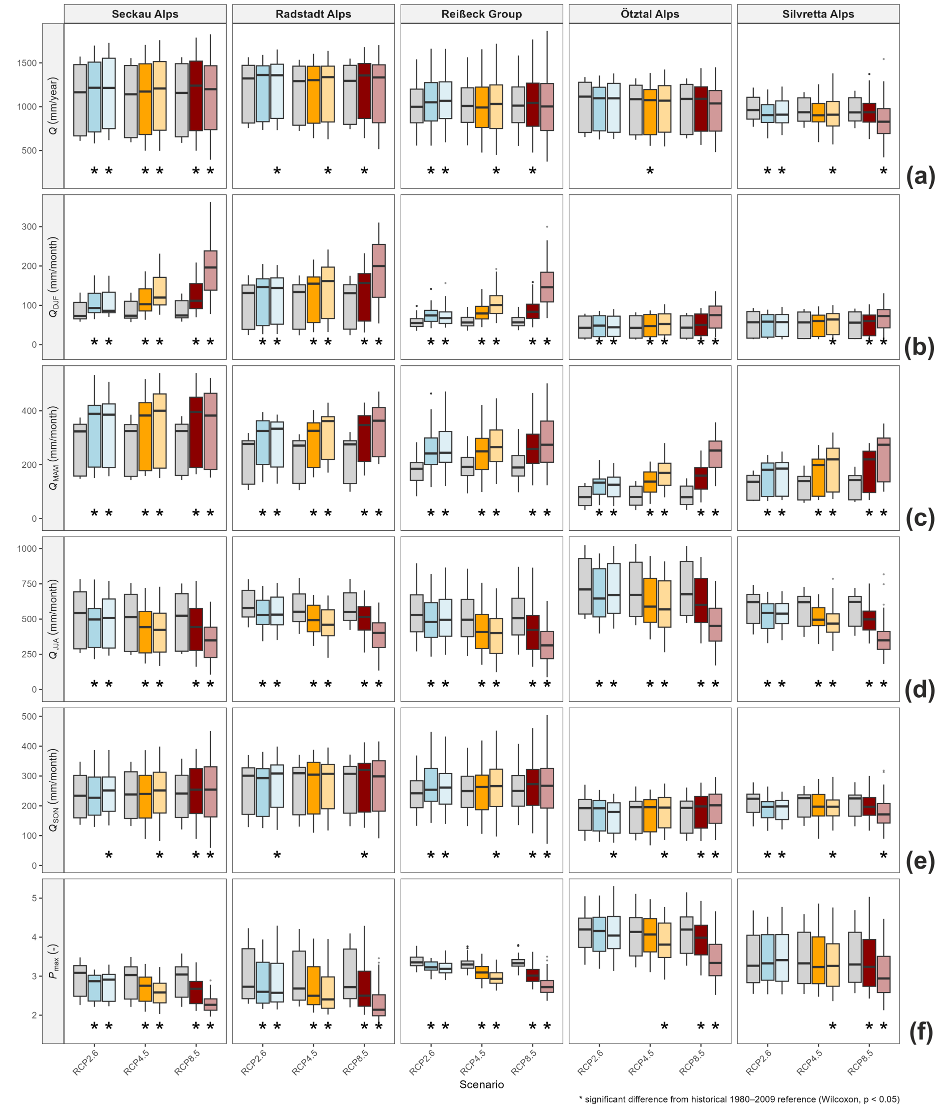

Figure 6. Seasonal and annual discharge indices across the five study sites. Boxplots illustrate the ensemble spread of hydrological indices for the historical reference period (1980–2009; grey), and two future periods: near-future (2030–2059; saturated colors) and far-future (2070–2099; transparent colors). Results are disaggregated by emission scenario: RCP2.6 (blue), RCP4.5 (orange), and RCP8.5 (red). Rows represent (a) annual discharge normalized by catchment area (Q), (b) winter discharge (Q_{DJF}), (c) spring discharge (Q_{MAM}), (d) summer discharge (Q_{JJA}), (e) autumn discharge (Q_{SON}), and (f) maximum Pardé coefficient (P_{max}). Asterisks below the boxplots indicate that the difference between the respective future period and the historical reference is statistically significant at the α=0.05 level, based on the rank-sum test. Results are aggregated across all sub-catchments per study site to show regional sensitivity to climatic forcing.

https://doi.org/10.5194/egusphere-2026-3664
Preprint. Discussion started: 22 July 2026

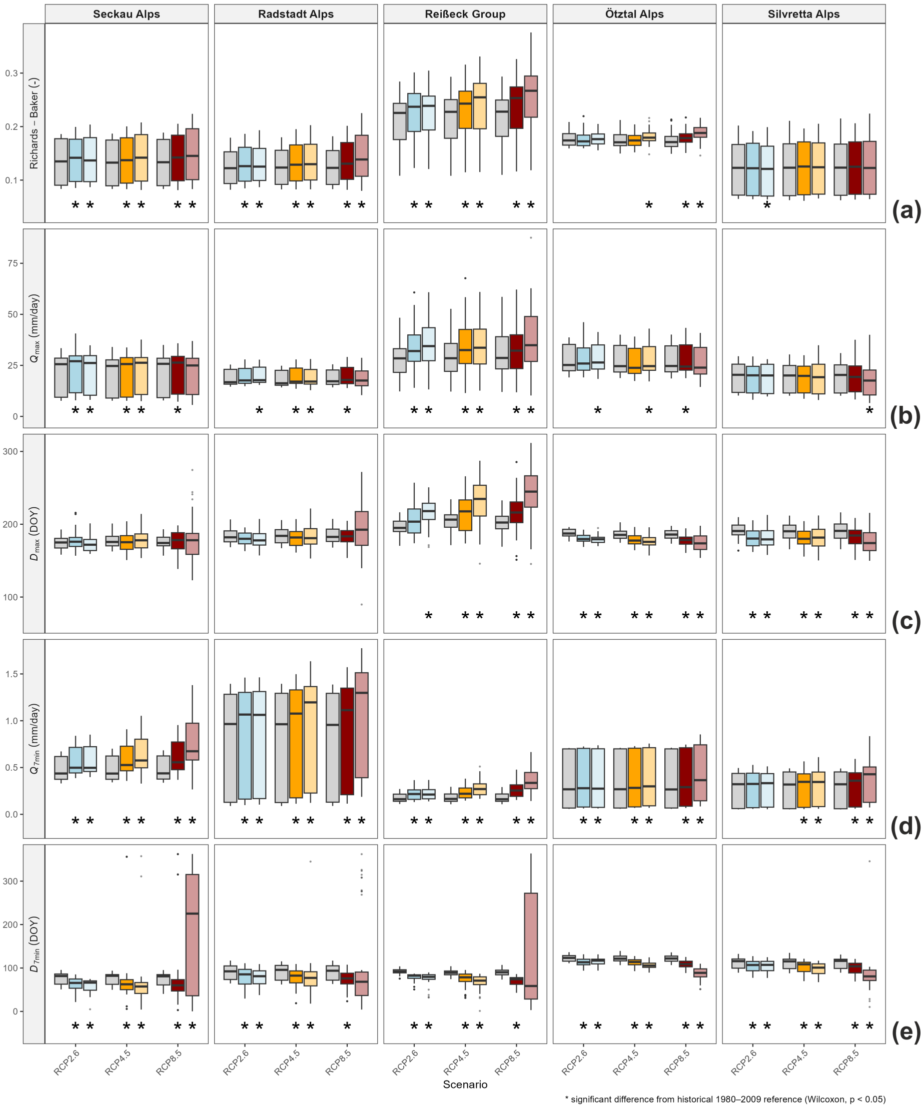

Figure 7. Changes in runoff dynamics across the five study sites, quantified by Richards-Baker flashiness index (*RB*), annual maximum flow (Q_{max}) and its timing (D_{max}), as well as annual minimum 7-day low flow (Q_{7min}) and its timing (D_{7min}). Boxplots illustrate the ensemble spread for the historical reference period (1980–2009; grey), and the projected shifts for the near-future (2030–2059; saturated colors) and far-future (2070–2099; transparent colors) periods. Results are disaggregated by emission scenario: RCP2.6 (blue), RCP4.5 (orange), and RCP8.5 (red). Asterisks below the boxplots denote statistically significant differences between the future period and the historical reference at the α=0.05 level, determined by the rank-sum test.

From a process-oriented perspective, this shift closely mirrors a distinct altitudinal gradient in temperature sensitivity (Supplementary Figure S36c). In mid-altitude catchments, winter discharge increases as temperatures more frequently exceed

https://doi.org/10.5194/egusphere-2026-3664
Preprint. Discussion started: 22 July 2026

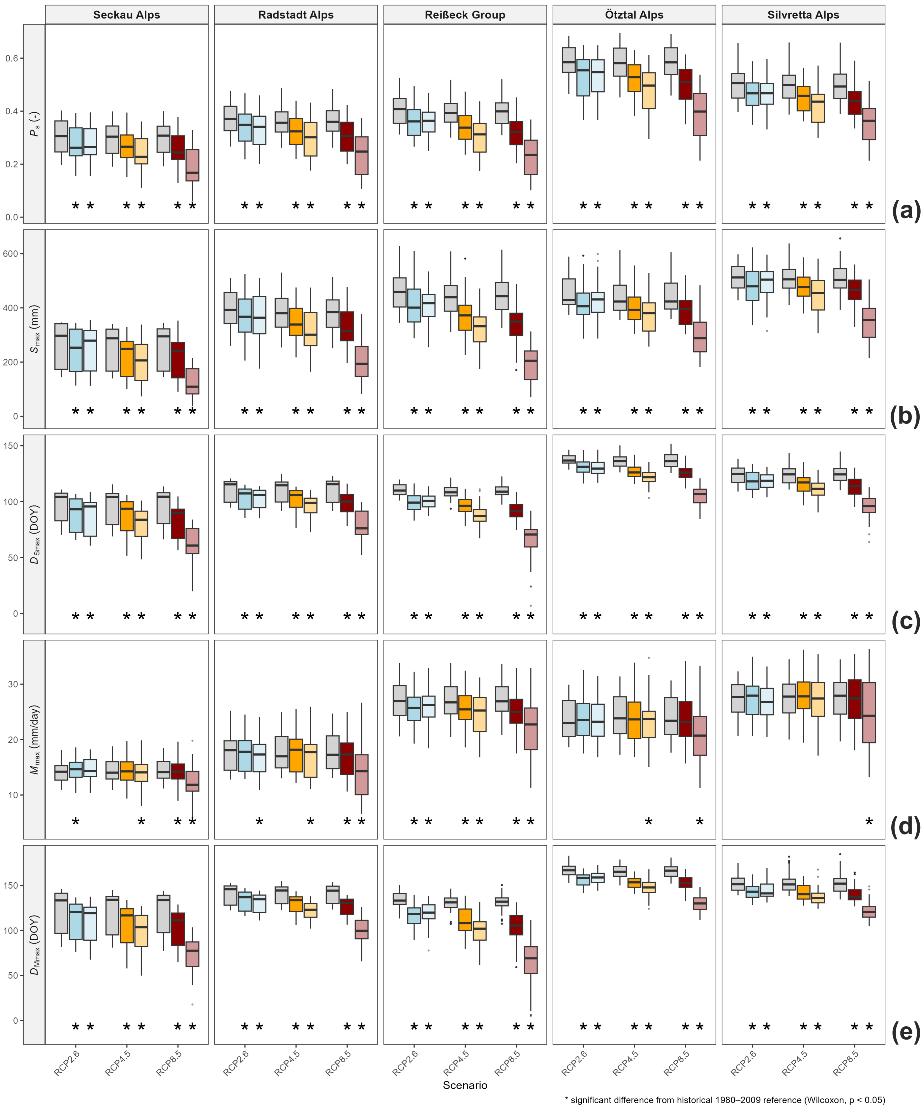

Figure 8. Changes in snow cover and melt dynamics across the five study sites. Boxplots illustrate the ensemble spread for the historical reference period (1980–2009; grey), and the projected shifts for the near-future (2030–2059; saturated colors) and far-future (2070–2099; transparent colors) periods. Results are disaggregated by emission scenario: RCP2.6 (blue), RCP4.5 (orange), and RCP8.5 (red). Columns represent (a) snow fraction of precipitation (P_s), (b) annual maximum snow water equivalent (S_{max}), (c) timing of maximum snow water equivalent (D_{Smax}), (d) maximum daily snowmelt rate (M_{max}), and (e) timing of maximum daily melt (D_{Mmax}). Asterisks below the boxplots denote statistically significant differences between the future period and the historical reference at the α=0.05 level, determined by the rank-sum test. These metrics characterize the shifting 'water tower' function of the alpine snowpack, highlighting trends toward reduced storage and advanced melt phenology.

0°C, triggering higher rainfall fractions and episodic melt events, whereas at high altitudes, temperatures stay sufficiently low to retain most precipitation as snow (similar to findings by Morán-Tejeda et al., 2013; Sospedra-Alfonso et al., 2015; Speich et al., 2015; Haslinger et al., 2023). The significant rise in spring discharge and universal reduction in summer flows are in line with projected changes in alpine runoff elsewhere; higher temperatures shift the onset of snowmelt and streamflow to earlier in the season, which, combined with earlier melt-out, leads to subsequent declines in summer flows (e.g., Barnhart et al., 2016; Jenicek et al., 2016, 2018; Brahney et al., 2017; Blahušiaková et al., 2020). By gradually losing the capacity for seasonal water storage in the snowpack, these trends diminish runoff seasonality and highlight a seasonal reorganization of hydrological regimes.

Changes in runoff flashiness and extreme flows, illustrated in Figure 7 and detailed in Supplementary Table S2, further underscore the transition toward more responsive hydrological regimes. The Richards-Baker flashiness index (*RB*) increases significantly across the mid-altitude catchments of the Seckau Alps, Radstadt Alps, and Reißeck Group, reflecting a tendency toward more rapid hydrological response times (Figure 7a). Interestingly, these increases in flashiness occur precisely where the overall discharge seasonality (P_{max}) declines most sharply (Figure 6f). Conversely, high-elevation catchments in the Ötztal and Silvretta Alps maintain a more stable P_{max} and generally show no significant increases in *RB*. This suggests that the loss of seasonal snow buffering—driven by rising rainfall fractions and declining snow storage—forces mid-altitude catchments to respond more rapidly to meteorological forcing as they transition from snow- to rain-dominated regimes. Similar to our results, such an acute sensitivity has been reported for mid-altitude catchments in several studies (Speich et al., 2015; Blahušiaková et al., 2020; Hotovy et al., 2025).

This heightened flashiness translates directly into an intensification of annual high flows (Q_{max}), which increase significantly across most mid-altitude catchments and scenarios without a clear shift in timing (Figure 7b, c). Conversely, high-altitude catchments exhibit no clear change in Q_{max} magnitude, but show a distinct shift toward earlier annual maximum flows. This divergence suggests that while mid-altitude catchments are primarily sensitive to increased rainfall intensity, high-altitude systems are dominated by the thermal shift toward earlier snowmelt.

Concurrently, annual low flows (Q_{7min}) increase, indicating a general reduction in low-flow severity and a shortening of the traditional winter low-flow period due to more frequent interruptions by episodic melt and rainfall events (Figure 7d). Changes in both annual maximum flows and annual 7-day low flows exhibit no systematic dependence on the percentage of catchment area drained through rock glaciers (Supplementary Figure S38). Conversely, downstream catchments with extensive karst aquifers or valley-fill sediments—such as Hammerjäger (Seckau Alps), Mauterndorf (Radstadt Alps), and Gargellen (Silvretta Alps)—exhibit a greater capacity to dampen these extreme responses, displaying attenuated changes in both magnitude and timing (Supplementary Figure S38).

Low-flow timing advances by 1–3 weeks across most catchments and scenarios (Figure 7e), yet remains concentrated in winter. This implies that freezing and snowmelt processes will continue to dominate future low-flow regimes. Only a few catchments under RCP 8.5 in the far future show a incipient transition toward summer low flows. While such shifts from winter to summer low flows are already anticipated for lower-elevation and pre-alpine catchments due to earlier melt-out, moisture deficits, and increased evaporation (Laaha et al., 2016; Jenicek et al., 2016, 2018; Hanus et al., 2021), our results suggest

https://doi.org/10.5194/egusphere-2026-3664
Preprint. Discussion started: 22 July 2026

that this transition likely occurs downstream from our relatively small high-alpine and mid-altitude headwaters. However, the strong summer flow declines in our data suggest that these headwaters are following the same trajectory, though exhibiting a delayed response compared to lower-elevation streams.

Snow indices show strong and consistent declines in snow storage across all catchments, emission scenarios, and periods (Figure 8, Supplementary Table S3). The fraction of solid precipitation (P_s) decreases significantly, with this downward trend intensifying under higher emission scenarios and toward the end of the century (Figure 8a). Despite differing absolute levels, mid- and high-altitude catchments show similarly strong reductions: while P_s remains consistently higher in high-altitude catchments of the Ötztal and Silvretta Alps—indicating that snow continues to play a dominant hydrological role—these systems experience substantial reductions, whereas in mid-altitude catchments the marked decline implies a progressive loss of snow relevance. A similar elevation gradient is evident within individual basins, with headwater regions retaining higher snow fractions than downstream reaches across all study sites (Supplementary Figures S39–S43).

Annual maximum snow water equivalent (S_{max}) decreases significantly everywhere, and its timing (D_{Smax}) shifts systematically earlier in the year (Figure 8b,c). This indicates both a reduction in peak snow accumulation and an advance in the seasonal snow cycle, reflecting earlier onset of melt. Again, these changes show a consistent elevational gradient, with higher-altitude and upstream areas retaining larger S_{max} and later timing than lower-altitude and downstream regions, but the magnitude of shifts is similar across elevations (Supplementary Table S3, Supplementary Figures S39–S43). In addition, snow cover duration (S_{dur}) decreases significantly across all catchments, indicating a shortening of the snow season from both reduced accumulation and earlier melt-out (Supplementary Figure S36d). This is accompanied by a consistent increase in air temperature (AT) and positive degree-day sums (PDD), pointing to a strong temperature-driven influence on these changes (Supplementary Figure S36c,e). Similar changes in snow dynamics are observed in other mountain catchments (e.g., Sospedra-Alfonso et al., 2015; Marty et al., 2017; Jenicek et al., 2018) and have been identified as a primary driver of reduced summer runoff due to diminished groundwater recharge from snowmelt (Beaulieu et al., 2012; Teutschbein et al., 2015; van Loon et al., 2015; Barnhart et al., 2016; Jenicek et al., 2016; Brahney et al., 2017).

Changes in snowmelt dynamics are more differentiated but remain secondary to the dominant signal of declining storage. The maximum daily snowmelt rate (M_{max}) shows a decreasing tendency, although this pattern is inconsistent across catchments and frequently lacks statistical significance (Figure 8d). This suggests that enhanced atmospheric energy input (increasing AT and PDD) does not compensate for reduced snow availability (decreasing S_{max} and S_{dur}). While a warmer atmosphere provides the thermal energy for more rapid snowmelt, the decreasing total snow water equivalent offsets these effects and prevents a clear directional change in maximum snowmelt rates. In addition, total annual snowmelt decreases significantly, reflecting the overarching loss of seasonal snow storage (Supplementary Figure S36f). The observed shift toward earlier onset of snowmelt (Figure 8e) further dampens melt rates due to lower early-spring radiation compared to late spring and early summer (Musselman et al., 2017).

These indices reveal a fundamental reorganization of the hydrological cycle toward a more rapid and seasonally advanced regime. The broad reduction in snow storage marks a shift from prolonged seasonal retention to immediate runoff, which cannot be compensated by the natural buffering capacity of most headwater aquifers. While these trends establish a new baseline for

https://doi.org/10.5194/egusphere-2026-3664
Preprint. Discussion started: 22 July 2026

seasonal timing, the resulting acceleration of the water cycle suggests an increased sensitivity to hydrological imbalances. We therefore investigate how this reorganization translates into a shift in the return period of extremes, focusing on the changing frequency and intensity of anomalous hydrometeorological events.

4.4 Shifts in Event Frequency and Hydrological Extremes

We assess changes in extreme events by analyzing how the return periods of historical 10-year events shift under future conditions, expressed as frequency amplification factors. Boxplots summarize the ensemble spread across all catchments per study site, and statistically significant changes ($\alpha = 0.05$) are indicated by an asterisk below the respective boxplots (Figure 9; corresponding HL estimates and p-values are provided in Supplementary Table S4). The full results for individual catchments are provided in Supplementary Figures S44–S48.

For snow-rich winters (Figure 9a), a clear and robust signal emerges: their frequency decreases significantly across nearly all catchments and scenarios. Under strong climate forcing (RCP8.5, far future), amplification factors approach zero, indicating that such snow-rich winters virtually disappear. Only under weaker forcing (RCP2.6) do snow-rich years persist, with occasional minor, statistically non-significant increases reflecting slightly wetter but not substantially warmer conditions (Haslinger et al., 2023; Kotlarski et al., 2023).

In contrast, extreme daily snowmelt shows no consistent overall trend (Figure 9b). Although atmospheric drivers of melt increase significantly, declining snow availability offsets this effect, resulting in a mixed response. A weak pattern is evident, with slight increases in the near future under low-emission scenarios and decreases in the far future under high-emission scenarios, but most changes are not statistically significant. This competing interplay varies systematically along elevation gradients; for instance, in the Seckau Alps, extreme snowmelt shows minor changes at the upstream Kettentörlquelle catchment but decreases strongly downstream at Hammerjäger, a topographic gradient mirrored across our other study sites (Supplementary Figures S44–S48).

Our analysis reveals a widespread and statistically significant increase in rain-on-snow events (Figure 9c). Typically, event frequency amplifies by a factor of 1.3 to 2.8, with a median of 1.9. This transition is consistent with the earlier arrival of peak discharge, underscoring the sensitivity of alpine catchments to shifting snow dynamics. Despite the complex interplay of competing melt drivers, the overarching shift toward rain-dominated regimes serves as a driver of rain-on-snow frequency. In contrast to reported declines in lowland and pre-alpine catchments (e.g., Morán-Tejeda et al., 2016; Hotovy et al., 2023, 2025), the slight increase identified here likely reflects the high elevation of our study sites in the Austrian Alps. This suggests that the zone of strongest rain-on-snow influence on streamflow extremes may shift toward higher elevations under continued warming (consistent with findings of Musselman et al., 2018; Li et al., 2019; López-Moreno et al., 2021), with changes in high-alpine rain-on-snow regimes continuing to propagate downstream and potentially contribute to flood hazards along the hydrological cascade.

Transforming these changes into runoff extremes, high flows tend to increase in frequency across most study sites, although the signal is weaker in high-elevation western catchments of the Ötztal and Silvretta Alps, exhibiting a median increase of 1.1 (Figure 9d). In contrast, mid-altitude catchments show a more pronounced response, with a median frequency increase of

https://doi.org/10.5194/egusphere-2026-3664
Preprint. Discussion started: 22 July 2026

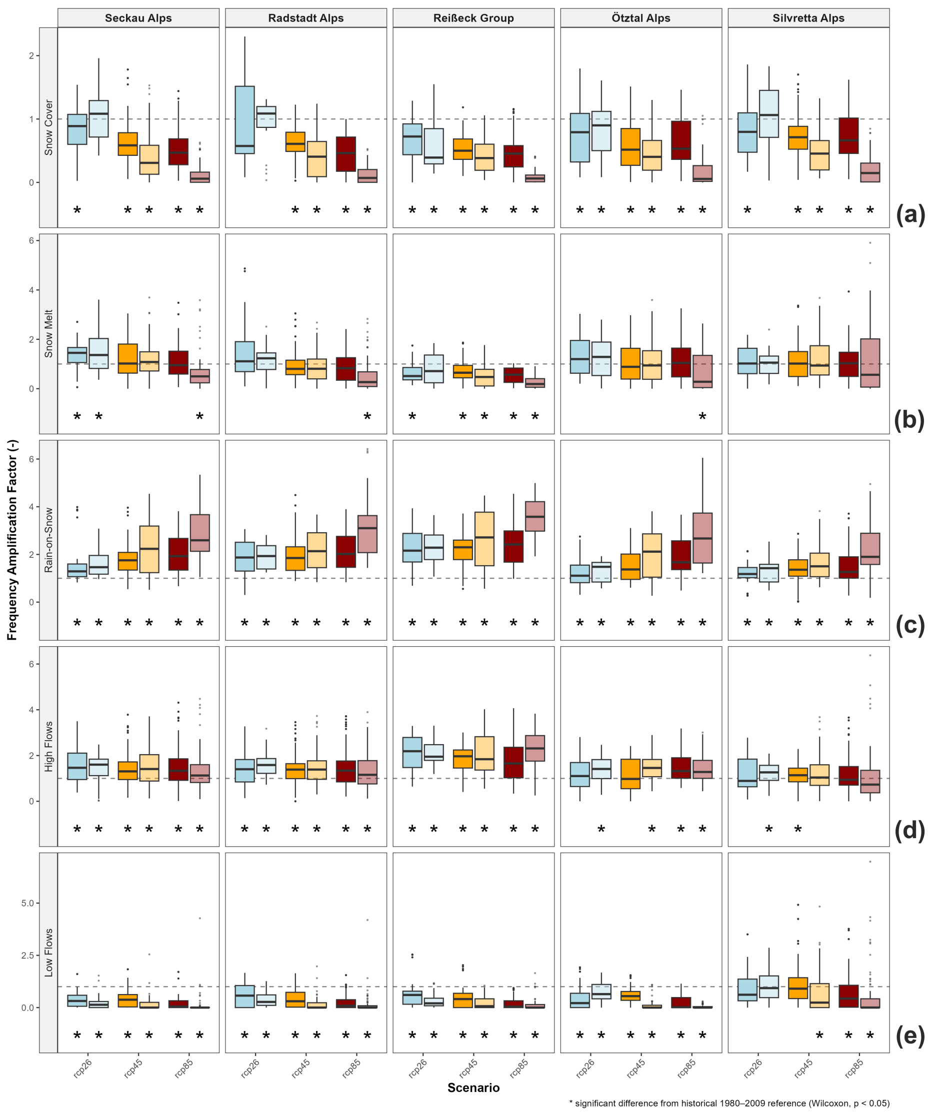

Figure 9. Change in the frequency of historical 10-year events based on annual extreme value analysis. Values are expressed as the frequency amplification factor, indicating the projected change in the likelihood of historical (1980–2009) events under future climate conditions. Results are disaggregated by emission scenario—RCP2.6 (blue), RCP4.5 (orange), and RCP8.5 (red)—and by time horizon: near-future (2030–2059; saturated colors) and far-future (2070–2099; transparent colors). Analyzed variables include: (a) snow cover (maximum catchment-wide snow water equivalent), (b) snowmelt (maximum daily melt rate), (c) high flows (annual maximum spring and river discharge), and (d) low flows (annual minimum 7-day discharge). Boxplots depict the ensemble spread across all climate model runs per RCP. Asterisks below the boxplots indicate that the shift in frequency is statistically significant at the α=0.05 level based on a rank-sum test.

https://doi.org/10.5194/egusphere-2026-3664
Preprint. Discussion started: 22 July 2026

1.5. Again, this this reflects a transition from snow-dominated storage toward immediate runoff generation that is especially pronounced at mid-altitudes, heightening the risk of high-flow events; periods once defined by snow accumulation are now more frequently influenced by rainfall and rain-on-snow processes, which trigger more rapid hydrological responses and promote widespread flooding (Morán-Tejeda et al., 2016; Würzer et al., 2016; Hanus et al., 2021; Hotovy et al., 2023, 2025).

In contrast, low-flow events become less frequent across nearly all catchments (Figure 9e). Across the study sites, event frequency drops to a median of 0.14, with these events vanishing entirely in more than one-third of the catchments. This aligns with the observed shifts in seasonal water availability, predominantly increasing winter and spring flows due to earlier snowmelt. Across the catchments studied, low flows are largely driven by winter drought conditions, when recharge is limited due to snow storage. Under future warming, shorter snow cover duration and increased winter rainfall and melt lead to enhanced recharge, thereby reducing the occurrence of low-flow conditions. Further downstream, however, the emerging summer water deficit is expected to translate into intensified summer low flows—a trend projected to intensify with climate change, as demonstrated by several studies analyzing lower-elevation catchments (Godsey et al., 2014; Jenicek et al., 2016, 2018; Laaha et al., 2016; Arnoux et al., 2021).

In summary, while subsurface storage provides a localized buffer, it is increasingly overmatched by the pervasive loss of seasonal snow. Fragmented headwater aquifers, such as rock glaciers, lack the capacity to dampen this overarching cryospheric shift. Even larger downstream reservoirs, including karst systems and thick valley fills, cannot fully compensate for the widespread loss of snow storage. The resulting shift toward a flashier hydrological regime—defined by enhanced winter-spring recharge, advanced low-flow timing, and intensified summer deficits—signifies a fundamental reorganization of the alpine water cycle. As the loss of snow cover tightens the temporal coupling between precipitation and runoff, the system loses its characteristic seasonal buffering. Our results demonstrate that alpine aquifers lack the capacity to fully buffer these intensifying regime dynamics, resulting in a distinct shift in headwater runoff behavior.

5 Conclusions

This study assessed the climate sensitivity of alpine hydrology across 15 nested catchments in the Austrian Alps, representing a broad spectrum of climatic, topographic, and geological conditions. To this end, we calibrated a suite of hydrological models capable of simulating storage-release processes in snowpacks and alpine aquifers. These models were driven by an ensemble of 40 climate scenarios across three emission pathways (RCP 2.6, 4.5, and 8.5) to project changes in snow cover and runoff through the 21st century. By comparing near- and far-future horizons against a historical reference period, we quantified annual and seasonal changes in snow and runoff dynamics using hydrometeorological indices and extreme value analysis.

Our results demonstrate a systematic reorganization of the alpine hydrological cycle, where the temporal control of runoff is shifting from seasonal snow storage toward direct rainfall forcing. While annual discharge volumes remain relatively stable, a seasonal redistribution emerges across all scenarios, characterized by earlier spring peaks and significant summer deficits. This transition is driven by a decline in snow mass and a shortened snow season.

https://doi.org/10.5194/egusphere-2026-3664
Preprint. Discussion started: 22 July 2026

We find that the critical role of subsurface storage varies systematically along the upstream-downstream continuum. Small headwater catchments with limited storage—including those dominated by rock glacier debris—display the strongest shifts in seasonal runoff variation, whereas larger systems with substantial groundwater storage exhibit similar but markedly attenuated responses, highlighting the buffering role of thick valley-fill and karst aquifers. However, this subsurface storage cannot fully compensate for the diminishing attenuation provided by the snowpack, leading to a stronger temporal coupling between precipitation events and runoff generation, and more flashy catchment responses.

To fully resolve how these climate signals propagate along the hydrological cascade, future work must look beyond static baseline assumptions. Further downstream, rain-on-snow events will likely decline, and winter-dominated low flows will turn into severe summer low flows that worsen as climate change progresses. Addressing these shifting dynamics requires investigations to account for the dynamic, temporal evolution of aquifer properties: tracking how permafrost thaw, sediment redistribution, and changing land cover alter subsurface hydraulic characteristics over time will be key to deciphering how alpine catchments buffer water resources under ongoing climate change.

Code and data availability

Historical meteorological gridded datasets (SPARTACUS and ARET) were obtained from GeoSphere Austria (https://data.hub.geosphere.at/). Satellite-derived cryosphere products (MODIS) were retrieved from the National Snow and Ice Data Center (http://nsidc.org/daac/modis/index.html). Discharge data collected during extensive field campaigns in the upstream headwater catchments are openly accessible via Zenodo (Seelig et al., 2026b). Downstream discharge data from the Hydrographic Service of Austria are freely available from the Federal Ministry of Agriculture and Forestry, Climate and Environmental Protection, Regions and Water Management (ehyd.gv.at), while downstream datasets provided by TIWAG and illwerke vkw are subject to third-party restrictions and can be requested from the authors. The digital elevation model (DEM) was provided by Open Government Data Austria (https://www.data.gv.at). The rock glacier inventory used for catchment characterization is available from PANGAEA (Wagner et al., 2020a, c). Hydrological modeling was implemented in the R software environment (R Core Team, 2026) using the airGR package (Coron et al., 2017), both of which are available via the Comprehensive R Archive Network (https://cran.r-project.org/).

Appendix A: Model Plausibility Evaluation

Hydrological modeling showed good representative capacity, with results that are consistent within the nested catchment structure and align with physical site characteristics. Across the 15 calibrated models, KGE′ values range from 0.74 to 0.93, indicating acceptable model performance (Table A1). The individual performance components confirm a good reproduction of hydrograph dynamics, with strong correlations ($0.77 \leq r^2 \leq 0.94$), low bias ($1.01 \leq \beta \leq 1.05$), and realistic variance ratios ($0.99 \leq \gamma \leq 1.08$). Time series comparisons and additional diagnostic plots—including parity plots, flow duration curves, and seasonal regime analyses—are provided in Supplementary Figures S11–S25.

https://doi.org/10.5194/egusphere-2026-3664
Preprint. Discussion started: 22 July 2026

The calibrated parameter sets are consistent with both literature ranges and site-specific hydrogeological conditions. Snow model parameters fall within expected ranges for alpine environments, with θ_1 reflecting typical degree-day factors (1.4-5.5 mm/°C/day) and θ_2 capturing spatial variability in snowpack cold content related to terrain characteristics such as elevation, slope, and aspect (with values of ∼0.2-0.3 in small, uniformly exposed catchments (e.g., Arzkarquelle, Ochsenhütte) and ∼0.8-0.9 in larger, more heterogeneous catchments, where spatial climatic variability dampens the snow cover response to air temperature changes). The hysteresis parameters θ_3 and θ_4 reproduce the pronounced seasonal snow cover dynamics observed in the field (Figure 2, Table A1).

GR4J model parameters routing water through the catchments show clear spatial organization linked to physical catchment properties. The soil moisture storage capacity (x_1) is generally low in steep headwater catchments with limited soil development (∼10-30 mm), but increases in downstream valleys characterized by deeper soils, wetlands, and higher evapotranspiration (up to > 500 mm). Elevated x_1 values are also found in headwater catchments with significant open water storage (e.g., lakes or wetlands), reflecting the model structure in which evapotranspiration is controlled via the production store (e.g., x_1 = 242 mm at Buchleiten, where numerous small ponds and wetlands dominate the landscape, Supplementary Figure S5). One exception is the Rotbühel catchment, where an unusually high x_1 is attributed to a local ponding effect upstream of the gauging station (Supplementary Figure S8); here, a representative value (x_1 = 25 mm) was used for parameter transfer to the rock glacier catchments of the Silvretta Alps, while retaining the calibrated value for site-specific simulations.

The inter-catchment exchange parameter (x_2) reflects known hydrogeological settings, with positive values indicating inflows from beyond topographic boundaries in karstified systems (e.g., Postalm, Mauterndorf, Gargellen), while negative values are due to underflow not captured by gauging stations (e.g., Hammerjäger, Buchleiten, Ruppalm). The routing store capacity (x_3) and unit hydrograph time base (x_4) similarly align with expected storage and response characteristics: lower values in steep headwaters with limited storage, and higher values in valley systems with thick sedimentary fills and developed aquifers.

Downstream routing parameters are consistent with geomorphic controls on flow velocity. Calibrated celerities (c) reflect differences between diffuse flow over rugged terrain (e.g., Kettentörlbach) and more efficient routing along well-developed channel networks (e.g., Hammerjäger). Overall, the coherence between parameter values, model performance, and independent hydrogeological understanding supports the robustness and physical realism of the modeling approach.

Author contributions

Conceptualization: SS, MS, MV, TW, KK, MA, KH, RP, and GW. Data curation: SS, MS, MV, MM, MA, KH, HB, AL, MR, and GW. Formal analysis: SS, MS, MV, and MM. Investigation: SS, MS, MV, TW, MM, KK, MA, KH, HB, AL, MR, MO, MH, RP, and GW. Methodology: SS, MS, MV, MM, TW, MA, KH, and GW. Project administration: GW. Resources: TW, MA, KH, HB, AL, RMW, EÜ, and GW. Software: SS, MS, MV, and MM. Supervision: GW. Validation: SS, MS, MV, MM, TW, KK, MA, KH, RP, and GW. Visualization: SS and MS. Writing – original draft: SS, MS, MV, MM, and GW. Writing – review & editing: SS, MS, MV, TW, MM, KK, MA, KH, HB, AL, MR, MO, MH, RP, RMW, EÜ, and GW.

https://doi.org/10.5194/egusphere-2026-3664
Preprint. Discussion started: 22 July 2026

Table A1. Model results evaluated across 15 sub-catchments spanning five mountain ranges. Model performance metrics include modified Kling-Gupta efficiency KGE‘ (–), correlation coefficient r^2 (–), bias ratioβ (–), and variance ratio γ (–). Calibrated model parameters for the rainfall-runoff module (GR4J) include soil moisture accounting store capacity x_1 (mm), inter-catchment exchange coefficient x_2 (mm/day), routing store capacity x_3 (mm), and unit hydrograph time base x_4 (days). Calibrated parameters for the implemented snow module (CemaNeige) include degree-day factor θ_1 (mm/°C/day), cold-content factor θ_2 (–), and snow hysteresis parameters θ_3 (mm) and θ_4 (–).

Mountain Range	Catchment	KGE‘ (–)	r^2 (–)	β (–)	γ (–)	x_1 (mm)	x_2 (mm/day)	x_3 (mm)	x_4 (days)	c (m/s)	θ_1 (mm/°C/day)	θ_2 (–)	θ_3 (mm)	θ_4 (–)
Seckau Alps	Kettentörlquelle	0.86	0.87	1.01	0.99	31	7.1	150	2.1	–	1.4	0.69	24	0.06
Seckau Alps	Kettentörlbach	0.86	0.89	1.02	0.99	21	–0.5	30	1.2	0.03	4.3	0.97	14	1.00
Seckau Alps	Hammerjäger	0.76	0.81	1.04	1.08	371	–5.7	345	1.3	0.52	5.3	0.84	12	0.42
Radstadt Alps	Lantschfeldquelle	0.86	0.87	1.01	1.02	22	–6.9	401	1.6	–	2.3	0.93	30	0.06
Radstadt Alps	Postalm	0.74	0.77	1.05	1.06	194	1.9	8	2.4	0.02	3.0	0.98	34	0.25
Radstadt Alps	Mauterndorf	0.79	0.83	1.04	1.07	350	5.9	175	1.0	0.14	5.5	0.93	13	0.28
Reißeck Group	Buchleiten	0.83	0.84	1.01	1.04	242	–23.4	368	2.1		5.2	0.32	14	0.87
Reißeck Group	Ochsenhütte	0.86	0.87	1.01	1.03	179	1.8	77	1.2		5.4	0.23	8	0.92
Reißeck Group	Ruppalm	0.86	0.87	1.02	1.02	13	–6.8	159	1.4	0.09	4.3	0.75	14	0.88
Ötztal Alps	Arzkarquelle	0.91	0.92	1.02	1.00	18	5	119	2.1	–	4.2	0.27	34	0.31
Ötztal Alps	Vorderes Bergle	0.89	0.90	1.01	1.00	9	0.5	174	1.3	–	3.9	0.25	25	0.66
Ötztal Alps	Radurschlalpe	0.89	0.90	1.01	1.01	129	2	10	2.1	0.06	2.9	0.86	33	1.00
Silvretta Alps	Rotbühel	0.89	0.90	1.02	1.01	1688	–1.3	259	2.2	–	4.2	0.31	7	0.38
Silvretta Alps	Vergaldaalpe	0.93	0.94	1.01	1.01	21	–0.4	162	2.1	0.01	3.9	0.90	28	0.51
Silvretta Alps	Gargellen	0.89	0.91	1.02	1.02	537	2	54	2.2	0.01	4.0	0.90	9	0.53

https://doi.org/10.5194/egusphere-2026-3664
Preprint. Discussion started: 22 July 2026

Competing interests

The authors declare no conflict of interest.

Acknowledgements

We thank TIWAG–Tiroler Wasserkraft AG, illwerke vkw, the municipality of Spittal an der Drau, and the Hydrographic Services of the federal states of Carinthia, Salzburg, Styria, Tyrol, and Vorarlberg for providing supplementary data and for their support during fieldwork. We also extend our special thanks to Thomas Aigner, Michaela Arnhof, Günter Bichler, Maria Brandmayr, Andreas Brandstätter, Jutta Eybl, Michael Ferstl, Lisa Fischer, Michael Fritz, Stephan Hann, Sylke Hilberg, Harald Huemer, Andrina Janicke, Lukas Kohlmaier, Clemens Mathis, Thomas Nester, Bertram Netzer, Andreas Pilz, Claudia Puschenjak, Peter Rauch, Jochen Schlamberger, Johannes Schöber, Martin Schröttner, Barbara Stromberger, Bertold Uggowitzer, Josef Waldner, Josef Wieland, and Hans Wiesenegger for their expert advice and their assistance during fieldwork. This research was funded by the Austrian Federal Ministry of Agriculture and Forestry, Climate and Environmental Protection, Regions and Water Management and the federal provinces of Carinthia, Salzburg, Styria, Tyrol, and Vorarlberg within the DaFNE project RG-AlpCatch. The authors acknowledge the financial support by the University of Graz.

https://doi.org/10.5194/egusphere-2026-3664
Preprint. Discussion started: 22 July 2026

References

Arnoux, M., Brunner, P., Schaefli, B., Mott, R., Cochand, F., and Hunkeler, D.: Low-flow behavior of alpine catchments with varying quaternary cover under current and future climatic conditions, Journal of Hydrology, 592, 125 591, https://doi.org/10.1016/j.jhydrol.2020.125591, 2021.

Baker, D. B., Richards, R. P., Loftus, T. T., and Kramer, J. W.: A new flashiness index: Characteristics and applications to midwestern rivers and streams, JAWRA Journal of the American Water Resources Association, 40, 503–522, https://doi.org/10.1111/j.1752-1688.2004.tb01046.x, 2004.

Bard, A., Renard, B., Lang, M., Giuntoli, I., Korck, J., Koboltschnig, G., Janža, M., d'Amico, M., and Volken, D.: Trends in the hydrologic regime of Alpine rivers, Journal of Hydrology, 529, 1823–1837, https://doi.org/10.1016/j.jhydrol.2015.07.052, 2015.

Barnhart, T. B., Molotch, N. P., Livneh, B., Harpold, A. A., Knowles, J. F., and Schneider, D.: Snowmelt rate dictates streamflow, Geophysical Research Letters, 43, 8006–8016, https://doi.org/10.1002/2016GL069690, 2016.

Bearzot, F., Colombo, N., Cremonese, E., Di Cella, U. M., Drigo, E., Caschetto, M., Basiricò, S., Crosta, G. B., Frattini, P., Freppaz, M., Pogliotti, P., Salerno, F., Brunier, A., and Rossini, M.: Hydrological, thermal and chemical influence of an intact rock glacier discharge on mountain stream water, The Science of the total environment, 876, 162 777, https://doi.org/10.1016/j.scitotenv.2023.162777, 2023.

Beaulieu, M., Schreier, H., and Jost, G.: A shifting hydrological regime: A field investigation of snowmelt runoff processes and their connection to summer base flow, Sunshine Coast, British Columbia, Hydrological Processes, 26, 2672–2682, https://doi.org/10.1002/hyp.9404, 2012.

Beniston, M. and Stoffel, M.: Assessing the impacts of climatic change on mountain water resources, The Science of the total environment, 493, 1129–1137, https://doi.org/10.1016/j.scitotenv.2013.11.122, 2014.

Beniston, M., Farinotti, D., Stoffel, M., Andreassen, L. M., Coppola, E., Eckert, N., Fantini, A., Giacona, F., Hauck, C., Huss, M., Huwald, H., Lehning, M., López-Moreno, J.-I., Magnusson, J., Marty, C., Morán-Tejéda, E., Morin, S., Naaim, M., Provenzale, A., Rabatel, A., Six, D., Stötter, J., Strasser, U., Terzago, S., and Vincent, C.: The European mountain cryosphere: A review of its current state, trends, and future challenges, The Cryosphere, 12, 759–794, https://doi.org/10.5194/tc-12-759-2018, 2018.

Bentura, P. L. F. and Michel, C.: Flood routing in a wide channel with a quadratic lag-and-route method, Hydrological Sciences Journal, 42, 169–189, https://doi.org/10.1080/02626669709492018, 1997.

Berghuijs, W. R., Woods, R. A., and Hrachowitz, M.: A precipitation shift from snow towards rain leads to a decrease in streamflow, Nature Climate Change, 4, 583–586, https://doi.org/10.1038/nclimate2246, 2014.

Berghuijs, W. R., Hartmann, A., and Woods, R. A.: Streamflow sensitivity to water storage changes across Europe, Geophysical Research Letters, 43, 1980–1987, https://doi.org/10.1002/2016GL067927, 2016.

Berghuijs, W. R., Harrigan, S., Molnar, P., Slater, L. J., and Kirchner, J. W.: The Relative Importance of Different Flood–Generating Mechanisms Across Europe, Water Resources Research, 55, 4582–4593, https://doi.org/10.1029/2019WR024841, 2019.

Berthling, I.: Beyond confusion: Rock glaciers as cryo-conditioned landforms, Geomorphology, 131, 98–106, https://doi.org/10.1016/j.geomorph.2011.05.002, 2011.

Bertolotti, G., Vremec, M., Seelig, S., Krainer, K., Wagner, T., Fischer, A., and Winkler, G.: Characterization of recharge components for delineation of a high-alpine rock glacier spring catchment, Ötztal Alps (northern Italy), Hydrogeology Journal, 12, 48, https://doi.org/10.1007/s10040-025-03005-y, 2026.

https://doi.org/10.5194/egusphere-2026-3664
Preprint. Discussion started: 22 July 2026

Blahušiaková, A., Matoušková, M., Jenicek, M., Ledvinka, O., Kliment, Z., Podolinská, J., and Snopková, Z.: Snow and climate trends and their impact on seasonal runoff and hydrological drought types in selected mountain catchments in Central Europe, Hydrological Sciences Journal, 65, 2083–2096, https://doi.org/10.1080/02626667.2020.1784900, 2020.

Blöschl, G., Sivapalan, M., Wagener, T., Viglione, A., and Savenije, H.: Runoff Prediction in Ungauged Basins: Synthesis across Processes, Places and Scales, Cambridge University Press, Cambridge, 2013.

Blöschl, G., Hall, J., Parajka, J., Perdigão, R. A. P., Merz, B., Arheimer, B., Aronica, G. T., Bilibashi, A., Bonacci, O., Borga, M., Čanjevac, I., Castellarin, A., Chirico, G. B., Claps, P., Fiala, K., Frolova, N., Gorbachova, L., Gül, A., Hannaford, J., Harrigan, S., Kireeva, M., Kiss, A., Kjeldsen, T. R., Kohnová, S., Koskela, J. J., Ledvinka, O., Macdonald, N., Mavrova-Guirguinova, M., Mediero, L., Merz, R., Molnar, P., Montanari, A., Murphy, C., Osuch, M., Ovcharuk, V., Radevski, I., Rogger, M., Salinas, J. L., Sauquet, E., Šraj, M., Szolgay, J., Viglione, A., Volpi, E., Wilson, D., Zaimi, K., and Živković, N.: Changing climate shifts timing of European floods, Science, 357, 588–590, https://doi.org/10.1126/science.aan2506, 2017.

Brahney, J., Menounos, B., Wei, X., and Curtis, P. J.: Determining annual cryosphere storage contributions to streamflow using historical hydrometric records, Hydrological Processes, 31, 1590–1601, https://doi.org/10.1002/hyp.11128, 2017.

Brighenti, S., Tolotti, M., Bruno, M. C., Engel, M., Wharton, G., Cerasino, L., Mair, V., and Bertoldi, W.: After the peak water: The increasing influence of rock glaciers on alpine river systems, Hydrological Processes, 33, 2804–2823, https://doi.org/10.1002/hyp.13533, 2019a.

Brighenti, S., Tolotti, M., Bruno, M. C., Wharton, G., Pusch, M. T., and Bertoldi, W.: Ecosystem shifts in Alpine streams under glacier retreat and rock glacier thaw: A review, The Science of the total environment, 675, 542–559, https://doi.org/10.1016/j.scitotenv.2019.04.221, 2019b.

Brighenti, S., Delpero, M., Bearzot, F., Bertolotti, G., Tolotti, M., Bruno, M. C., Fischer, A., Winkler, G., Voto, G., Aguzzoni, A., Tirler, W., and Comiti, F.: Cryosphere and lithology influence the hydrological gradients of high elevation Alpine catchments, Catena, 263, 109 676, https://doi.org/10.1016/j.catena.2025.109676, 2026.

Brunner, M. I. and Fischer, S.: Snow-influenced floods are more strongly connected in space than purely rainfall-driven floods, Environmental Research Letters, 17, 104 038, https://doi.org/10.1088/1748-9326/ac948f, 2022.

Chartier-Rescan, C., Wood, R. R., and Brunner, M. I.: Snow drought propagation and its impacts on streamflow drought in the Alps, Environmental Research Letters, 20, 054 032, https://doi.org/10.1088/1748-9326/adc824, 2025.

Chimani, B., Heinrich, G., Hofstätter, M., Kerschbaumer, M., Kienberger, S., Leuprecht, A., Lexer, A., Peßenteiner, S., Poetsch, M. S., Salzmann, M., Spiekermann, R., Switanek, M., and Truhetz, H.: ÖKS 15 Klimaszenarien für Österreich: Daten - Methoden - Klimaanalyse.

Chimani, B., Matulla, C., Hiebl, J., Schellander-Gorgas, T., Maraun, D., Mendlik, T., Eitzinger, J., Kubu, G., and Thaler, S.: Compilation of a guideline providing comprehensive information on freely available climate change data and facilitating their efficient retrieval, Climate Services, 19, 100 179, https://doi.org/10.1016/j.cliser.2020.100179, 2020.

Chin, D. A.: Water-Resources Engineering: International Edition, Pearson Education, Boston, Mass., 3 edn., 2013.

Citrini, A., Camera, C., and Beretta, G. P.: Nossana Spring (Northern Italy) under Climate Change: Projections of Future Discharge Rates and Water Availability, Water, 12, 387, https://doi.org/10.3390/w12020387, 2020.

Cliff, R. A., Norris, R. J., Oxburgh, E. R., and Wright, R. C.: Structural, Metamorphic and Geochronological Studies in the Reisseck and Southern Ankogel Groups, the Eastern Alps, Jahrbuch der Geologischen Bundesanstalt, 114, 121–272, 1971.

Coron, L., Thirel, G., Delaigue, O., Perrin, C., and Andréassian, V.: The suite of lumped GR hydrological models in an R package, Environmental Modelling & Software, 94, 166–171, https://doi.org/10.1016/j.envsoft.2017.05.002, 2017.

Exner, C.: Geologie der Hohen Tauern bei Gmünd in Kärnten, Jahrbuch der Geologischen Bundesanstalt, 123, 343–410, 1980.

Exner, C.: Der Südrand des Tauernfensters bei Spittal an der Drau, Jahrbuch der Geologischen Bundesanstalt, 127, 349–367, 1984.

Exner, C.: Geologie des mittleren Lungaus, Jahrbuch der Geologischen Bundesanstalt, 132, 7–103, 1989.

Exner, C., Hejl, E., and Mandl, G. W.: Geologische Karte der Republik Österreich 1:50 000: Blatt 157 Tamsweg, 2005.

Godsey, S. E., Kirchner, J. W., and Tague, C. L.: Effects of changes in winter snowpacks on summer low flows: Case studies in the Sierra Nevada, California, USA, Hydrological Processes, 28, 5048–5064, https://doi.org/10.1002/hyp.9943, 2014.

Guo, Y., Yang, Y., Yang, D., Zhang, L., Zheng, H., Xiong, J., Ruan, F., Han, J., and Liu, Z.: Warming leads to both earlier and later snowmelt floods over the past 70 years, Nature communications, 16, 3663, https://doi.org/10.1038/s41467-025-58832-0, 2025.

Hanus, S., Hrachowitz, M., Zekollari, H., Schoups, G., Vizcaino, M., and Kaitna, R.: Future changes in annual, seasonal and monthly runoff signatures in contrasting Alpine catchments in Austria, Hydrology and Earth System Sciences, 25, 3429–3453, https://doi.org/10.5194/hess-25-3429-2021, 2021.

Harrington, J. S., Mozil, A., Hayashi, M., and Bentley, L. R.: Groundwater flow and storage processes in an inactive rock glacier, Hydrological Processes, 32, 3070–3088, https://doi.org/10.1002/hyp.13248, 2018.

Haslinger, K. and Bartsch, A.: Creating long-term gridded fields of reference evapotranspiration in Alpine terrain based on a recalibrated Hargreaves method, Hydrology and Earth System Sciences, 20, 1211–1223, https://doi.org/10.5194/hess-20-1211-2016, 2016.

Haslinger, K., Schöner, W., Abermann, J., Laaha, G., Andre, K., Olefs, M., and Koch, R.: Apparent contradiction in the projected climatic water balance for Austria: Wetter conditions on average versus higher probability of meteorological droughts, Natural Hazards and Earth System Sciences, 23, 2749–2768, https://doi.org/10.5194/nhess-23-2749-2023, 2023.

Hauer, C., Paster, M., Pulg, U., Ofenböck, T., and Habersack, H.: Critical flows at the Wien River during the 1000-years event in September 2024 – causes, consequences and possible management options for urban river flood management, Natural Hazards, 121, 11 173–11 185, https://doi.org/10.1007/s11069-025-07244-w, 2025.

Häusler, H.: Geologische Karte der Republik Österreich 1:50 000: Blatt 156 Muhr, 1995.

Hayashi, M.: Alpine Hydrogeology: The Critical Role of Groundwater in Sourcing the Headwaters of the World, Ground Water, 58, 498–510, https://doi.org/10.1111/gwat.12965, 2020.

Helsel, D. R., Hirsch, R. M., Ryberg, K. R., Archfield, S. A., and Gilroy, E. J.: Statistical Methods in Water Resources, vol. book 4, chapter A3 of *U. S. Geol. Surv. Techniques and Methods*, U. S. Geological Survey (USGS), Reston, https://doi.org/10.3133/tm4A3, 2020.

Hiebl, J. and Frei, C.: Daily temperature grids for Austria since 1961—concept, creation and applicability, Theoretical and Applied Climatology, 124, 161–178, https://doi.org/10.1007/s00704-015-1411-4, 2016.

Hiebl, J. and Frei, C.: Daily precipitation grids for Austria since 1961—development and evaluation of a spatial dataset for hydroclimatic monitoring and modelling, Theoretical and Applied Climatology, 132, 327–345, https://doi.org/10.1007/s00704-017-2093-x, 2018.

Hock, R.: Temperature index melt modelling in mountain areas, Journal of Hydrology, 282, 104–115, https://doi.org/10.1016/S0022-1694(03)00257-9, 2003.

Hock, R., Rasul, G., Adler, C., Cáceres, B., Gruber, S., Hirabayashi, Y., Jackson, M., Kääb, A., Kang, S., Kutuzov, S., Milner, A., Molau, U., Morin, S., Orlove, B., and Steltzer, H.: High Mountain Areas, in: IPCC Special Report on the Ocean and Cryosphere in a Changing Climate, edited by Intergovernmental Panel on Climate Change, pp. 131–202, https://doi.org/10.1017/9781009157964.004, 2019.

Hodges, J. L. and Lehmann, E. L.: Estimates of Location Based on Rank Tests, The Annals of Mathematical Statistics, 34, 598–611, https://doi.org/10.1214/aoms/1177704172, 1963.

Hoinkes, G. and Thöni, M.: Evolution of the Ötztal-Stubai, Scarl-Campo and Ulten Basement Units, in: Pre-Mesozoic Geology in the Alps, edited by Raumer, J. F. and Neubauer, F., pp. 485–494, Springer Berlin Heidelberg, Berlin, Heidelberg, 1993.

Hollander, M., Wolfe, D. A., and Chicken, E.: Nonparametric statistical methods, Wiley series in probability and statistics, John Wiley & Sons Inc, Hoboken, New Jersey, 3 edn., https://doi.org/10.1002/9781119196037, 2014.

Hotovy, O., Nedelcev, O., and Jenicek, M.: Changes in rain-on-snow events in mountain catchments in the rain–snow transition zone, Hydrological Sciences Journal, 68, 572–584, https://doi.org/10.1080/02626667.2023.2177544, 2023.

Hotovy, O., Nedelcev, O., Seibert, J., and Jenicek, M.: Rain-on-snow events in mountainous catchments under climate change, Hydrology and Earth System Sciences, 29, 4199–4217, https://doi.org/10.5194/hess-29-4199-2025, 2025.

Immerzeel, W. W., Lutz, A. F., Andrade, M., Bahl, A., Biemans, H., Bolch, T., Hyde, S., Brumby, S., Davies, B. J., Elmore, A. C., Emmer, A., Feng, M., Fernández, A., Haritashya, U., Kargel, J. S., Koppes, M., Kraaijenbrink, P. D. A., Kulkarni, A. V., Mayewski, P. A., Nepal, S., Pacheco, P., Painter, T. H., Pellicciotti, F., Rajaram, H., Rupper, S., Sinisalo, A., Shrestha, A. B., Viviroli, D., Wada, Y., Xiao, C., Yao, T., and Baillie, J. E. M.: Importance and vulnerability of the world's water towers, Nature, 577, 364–369, https://doi.org/10.1038/s41586-019-1822-y, 2020.

Jacob, D., Petersen, J., Eggert, B., Alias, A., Christensen, O. B., Bouwer, L. M., Braun, A., Colette, A., Déqué, M., Georgievski, G., Georgopoulou, E., Gobiet, A., Menut, L., Nikulin, G., Haensler, A., Hempelmann, N., Jones, C., Keuler, K., Kovats, S., Kröner, N., Kotlarski, S., Kriegsmann, A., Martin, E., van Meijgaard, E., Moseley, C., Pfeifer, S., Preuschmann, S., Radermacher, C., Radtke, K., Rechid, D., Rounsevell, M., Samuelsson, P., Somot, S., Soussana, J.-F., Teichmann, C., Valentini, R., Vautard, R., Weber, B., and Yiou, P.: EURO-CORDEX: New high-resolution climate change projections for European impact research, Regional Environmental Change, 14, 563–578, https://doi.org/10.1007/s10113-013-0499-2, 2014.

Jenicek, M., Seibert, J., Zappa, M., Staudinger, M., and Jonas, T.: Importance of maximum snow accumulation for summer low flows in humid catchments, Hydrology and Earth System Sciences, 20, 859–874, https://doi.org/10.5194/hess-20-859-2016, 2016.

Jenicek, M., Seibert, J., and Staudinger, M.: Modeling of Future Changes in Seasonal Snowpack and Impacts on Summer Low Flows in Alpine Catchments, Water Resources Research, 54, 538–556, https://doi.org/10.1002/2017WR021648, 2018.

Jones, D. B., Harrison, S., Anderson, K., and Whalley, W. B.: Rock glaciers and mountain hydrology: A review, Earth-Science Reviews, 193, 66–90, https://doi.org/10.1016/j.earscirev.2019.04.001, 2019.

Kerschner, H.: Zeugen der Klimageschichte im oberen Radurschltal: Alte Gletscherstände und Blockgletscher in der Umgebung des Hohenzollernhauses, Zeitschrift des Deutschen und Österreichischen Alpenvereins, 107, 23–27, 1982.

Khaliq, M. N., Ouarda, T., Ondo, J.-C., Gachon, P., and Bobée, B.: Frequency analysis of a sequence of dependent and/or non-stationary hydro-meteorological observations: A review, Journal of Hydrology, 329, 534–552, https://doi.org/10.1016/j.jhydrol.2006.03.004, 2006.

Klein, G., Vitasse, Y., Rixen, C., Marty, C., and Rebetez, M.: Shorter snow cover duration since 1970 in the Swiss Alps due to earlier snowmelt more than to later snow onset, Climatic Change, 139, 637–649, https://doi.org/10.1007/s10584-016-1806-y, 2016.

Komma, J., Valent, P., Bertola, M., Parajka, J., Haslinger, K., Bica, B., Pistotnik, G., Breinl, K., Müller, G., Pavlin, L., Kahl, B., Naderer, A., and Blöschl, G.: The September 2024 Danube Flood Compared to the 1899, 2002, and 2013 Events: A Hydrometeorological Analysis in a Changing Climate, EGUsphere, 2025, 1–32, https://doi.org/10.5194/egusphere-2025-5435, 2025.

Kotlarski, S., Gobiet, A., Morin, S., Olefs, M., Rajczak, J., and Samacoïts, R.: 21st Century alpine climate change, Climate Dynamics, 60, 65–86, https://doi.org/10.1007/s00382-022-06303-3, 2023.

Laaha, G., Parajka, J., Viglione, A., Koffler, D., Haslinger, K., Schöner, W., Zehetgruber, J., and Blöschl, G.: A three-pillar approach to assessing climate impacts on low flows, Hydrology and Earth System Sciences, 20, 3967–3985, https://doi.org/10.5194/hess-20-3967-2016, 2016.

Laaha, G., Gauster, T., Tallaksen, L. M., Vidal, J.-P., Stahl, K., Prudhomme, C., Heudorfer, B., Vlnas, R., Ionita, M., van Lanen, H. A. J., Adler, M.-J., Caillouet, L., Delus, C., Fendekova, M., Gailliez, S., Hannaford, J., Kingston, D., van Loon, A. F., Mediero, L., Osuch, M., Romanowicz, R., Sauquet, E., Stagge, J. H., and Wong, W. K.: The European 2015 drought from a hydrological perspective, Hydrology and Earth System Sciences, 21, 3001–3024, https://doi.org/10.5194/hess-21-3001-2017, 2017.

Laghari, A. N., Vanham, D., and Rauch, W.: To what extent does climate change result in a shift in Alpine hydrology? A case study in the Austrian Alps, Hydrological Sciences Journal, 57, 103–117, https://doi.org/10.1080/02626667.2011.637040, 2011.

Lavenne, A., Andréassian, V., Thirel, G., Ramos, M.-H., and Perrin, C.: A Regularization Approach to Improve the Sequential Calibration of a Semidistributed Hydrological Model, Water Resources Research, 55, 8821–8839, https://doi.org/10.1029/2018WR024266, 2019.

Lerat, J., Andréassian, V., Perrin, C., Vaze, J., Perraud, J. M., Ribstein, P., and Loumagne, C.: Do internal flow measurements improve the calibration of rainfall-runoff models?, Water Resources Research, 48, W02 511, https://doi.org/10.1029/2010WR010179, 2012.

Li, D., Lettenmaier, D. P., Margulis, S. A., and Andreadis, K.: The Role of Rain–on–Snow in Flooding Over the Conterminous United States, Water Resources Research, 55, 8492–8513, https://doi.org/10.1029/2019WR024950, 2019.

Lobligeois, F., Andréassian, V., Perrin, C., Tabary, P., and Loumagne, C.: When does higher spatial resolution rainfall information improve streamflow simulation? An evaluation using 3620 flood events, Hydrology and Earth System Sciences, 18, 575–594, https://doi.org/10.5194/hess-18-575-2014, 2014.

López-Moreno, J. I., Pomeroy, J. W., Morán-Tejeda, E., Revuelto, J., Navarro-Serrano, F. M., Vidaller, I., and Alonso-González, E.: Changes in the frequency of global high mountain rain-on-snow events due to climate warming, Environmental Research Letters, 16, 094 021, https://doi.org/10.1088/1748-9326/ac0dde, 2021.

Mandl, G. W. and Matura, A.: Geologische Karte der Republik Österreich 1:50 000: Blatt 127 Schladming, 1995.

Mandl, M., Kurz, W., Hauzenberger, C., Fritz, H., Klötzli, U., and Schuster, R.: Pre-Alpine evolution of the Seckau Complex (Austroalpine basement/Eastern Alps): Constraints from in-situ LA-ICP-MS U Pb zircon geochronology, Lithos, 296-299, 412–430, https://doi.org/10.1016/j.lithos.2017.11.022, 2018.

Mandl, M., Kurz, W., Hauzenberger, C., Fritz, H., and Pfingstl, S.: Geochemistry of granitoids from the Austroalpine Seckau Complex: A key for revealing the pre-Alpine evolution of the Eastern Alps, Mineralogy and Petrology, 116, 251–272, https://doi.org/10.1007/s00710-022-00781-3, 2022.

Marty, C., Schlögl, S., Bavay, M., and Lehning, M.: How much can we save? Impact of different emission scenarios on future snow cover in the Alps, The Cryosphere, 11, 517–529, https://doi.org/10.5194/tc-11-517-2017, 2017.

Masten, M., Seelig, S., Vremec, M., Seelig, M., and Winkler, G.: An enhanced python framework for hydrological modeling in alpine catchments: Snow hysteresis and glacier ice melt, Environmental Modelling & Software, 197, 106 842, https://doi.org/10.1016/j.envsoft.2025.106842, 2026.

Masten, M., Seelig, M., Seelig, S., Vremec, M., Wagner, T., Obwegs, M., Hausleber, M., Eybl, J., and Winkler, G.: Climate Change Impacts on Alpine Springs in Austria: Shifts in Discharge Seasonality and Water Availability, Journal of Hydrology, under review.

Mathis, C.: Die Fidelisquelle, in: Quellbeobachtung im Hydrographischen Dienst in Österreich, edited by Bundesministerium für Land- und Forstwirtschaft, Umwelt und Wasserwirtschaft, Mitteilungen des Hydrographischen Zentralbüros, pp. 59–65, Wien, 2005.

McMillan, H.: Linking hydrologic signatures to hydrologic processes: A review, Hydrological Processes, 34, 1393–1409, https://doi.org/10.1002/hyp.13632, 2020.

https://doi.org/10.5194/egusphere-2026-3664
Preprint. Discussion started: 22 July 2026

Meriö, L.-J., Ala-aho, P., Linjama, J., Hjort, J., Kløve, B., and Marttila, H.: Snow to Precipitation Ratio Controls Catchment Storage and Summer Flows in Boreal Headwater Catchments, Water Resources Research, 55, 4096–4109, https://doi.org/10.1029/2018WR023031, 2019.

Metz, K.: Der geologische Bau der Seckauer und Rottenmanner Tauern, Jahrbuch der Geologischen Bundesanstalt, 119, 151–205, 1976.

Morán-Tejeda, E., López-Moreno, J. I., and Beniston, M.: The changing roles of temperature and precipitation on snowpack variability in Switzerland as a function of altitude, Geophysical Research Letters, 40, 2131–2136, https://doi.org/10.1002/grl.50463, 2013.

Morán-Tejeda, E., López-Moreno, J. I., Stoffel, M., and Beniston, M.: Rain-on-snow events in Switzerland: Recent observations and projections for the 21st century, Climate Research, 71, 111–125, https://doi.org/10.3354/cr01435, 2016.

Moser, M.: GEOFAST 1:50 000. Zusammenstellung ausgewählter Archivunterlagen der Geologischen Bundesanstalt: Blatt 172 Weißkugel, 2012.

Moussu, F.: Prise en compte du fonctionnement hydrodynamique dans la modélisation pluie débit des systèmes karstiques, Dissertation, Université Pierre & Marie Curie, Paris, 2011.

Musselman, K. N., Clark, M. P., Liu, C., Ikeda, K., and Rasmussen, R.: Slower snowmelt in a warmer world, Nature Climate Change, 7, 214–219, https://doi.org/10.1038/nclimate3225, 2017.

Musselman, K. N., Lehner, F., Ikeda, K., Clark, M. P., Prein, A. F., Liu, C., Barlage, M., and Rasmussen, R.: Projected increases and shifts in rain-on-snow flood risk over western North America, Nature Climate Change, 8, 808–812, https://doi.org/10.1038/s41558-018-0236-4, 2018.

Oberhauser, R. and Rataj, W.: Geologisch-tektonische Übersichtskarte von Vorarlberg 1:200 000, 1998.

Ollivier, C., Mazzilli, N., Olioso, A., Chalikakis, K., Carrière, S. D., Danquigny, C., and Emblanch, C.: Karst recharge-discharge semi distributed model to assess spatial variability of flows, The Science of the total environment, 703, 134 368, https://doi.org/10.1016/j.scitotenv.2019.134368, 2020.

Open Government Data Austria: Digital Elevation Model of Austria, https://www.data.gv.at, accessed: 2026-06-22, 2025.

Paznekas, A. and Hayashi, M.: Groundwater contribution to winter streamflow in the Canadian Rockies, Canadian Water Resources Journal, 41, 484–499, 2016.

Perrin, C., Michel, C., and Andréassian, V.: Improvement of a parsimonious model for streamflow simulation, Journal of Hydrology, 279, 275–289, https://doi.org/10.1016/S0022-1694(03)00225-7, 2003.

Pestal, G., Rataj, W., Reitner, J. M., and Schuster, R.: Geologische Karte der Republik Österreich 1:50 000: Blatt 182 Spittal an der Drau, 2006.

Pfingstl, S., Kurz, W., Schuster, R., and Hauzenberger, C.: Geochronological constraints on the exhumation of the Austroalpine Seckau Nappe (Eastern Alps), Austrian Journal of Earth Sciences, 108, 172–185, 2015.

R Core Team: R: A Language and Environment for Statistical Computing, R Foundation for Statistical Computing, Vienna, Austria, https://doi.org/10.32614/R.manuals, 2026.

Ribis, M.: Geologisch-hydrogeologische und hydrochemische Untersuchungen in Permafrostbereichen der Ötztaler Alpen (Tirol, Österreich), Dissertation, Leopold-Franzens-Universität, Innsbruck, 2017.

Riboust, P., Thirel, G., Le Moine, N., and Ribstein, P.: Revisiting a Simple Degree-Day Model for Integrating Satellite Data: Implementation of Swe-Sca Hystereses, Journal of Hydrology and Hydromechanics, 67, 70–81, https://doi.org/10.2478/johh-2018-0004, 2019.

Riggs, G. A., Hall, D. K., and Román, M. O.: MODIS Snow Products Collection 6.1 User Guide: Version 1.0, 2019.

Schmid, S. M., Fügenschuh, B., Kissling, E., and Schuster, R.: Tectonic map and overall architecture of the Alpine orogen, Eclogae Geologicae Helvetiae, 97, 93–117, https://doi.org/10.1007/s00015-004-1113-x, 2004.

Schuster, R., Pestal, G., and Reitner, J. M.: Erläuterungen zu Blatt 182 Spittal an der Drau, Geologische Karte der Republik Österreich 1:50 000, Geologische Bundesanstalt, Wien, 2006.

Seelig, S., Seelig, M., Krainer, K., and Winkler, G.: Preferential flow paths in active rock glaciers, Earth-Science Reviews, 80, 105 373, https://doi.org/10.1016/j.earscirev.2025.105373, 2026a.

Seelig, S., Seelig, M., Vremec, M., Masten, M., Wagner, T., Krainer, K., Avian, M., Haslinger, K., Brielmann, H., Leis, A., Ribis, M., Obwegs, M., Hausleber, M., Philippitsch, R., Mauthner-Weber, R., Überreiter, E., and Winkler, G.: Daily Discharge Data from Rock Glacier Springs and Headwater Catchments, Austrian Alps, https://doi.org/10.5281/zenodo.20802643, 2026b.

Sezen, C., Bezak, N., Bai, Y., and Šraj, M.: Hydrological modelling of karst catchment using lumped conceptual and data mining models, Journal of Hydrology, 576, 98–110, https://doi.org/10.1016/j.jhydrol.2019.06.036, 2019.

Siirila-Woodburn, E. R., Thiros, N., Newcomer, M., Rudisill, W., Dennedy-Frank, P. J., Feldman, D., Sprenger, M., Carroll, R. W. H., Williams, K. H., and Brodie, E.: Warming and snow loss increase reliance on old groundwater in a Colorado River headwater, Nature Geoscience, 23, 32, https://doi.org/10.1038/s41561-026-01945-y, 2026.

Sölva, H., Grasemann, B., Thöni, M., Thiede, R., and Habler, G.: The Schneeberg Normal Fault Zone: Normal faulting associated with Cretaceous SE-directed extrusion in the Eastern Alps (Italy/Austria), Tectonophysics, 401, 143–166, https://doi.org/10.1016/j.tecto.2005.02.005, 2005.

Somers, L. D. and McKenzie, J. M.: A review of groundwater in high mountain environments, WIREs Water, 7, e1475, https://doi.org/10.1002/wat2.1475, 2020.

Sospedra-Alfonso, R., Melton, J. R., and Merryfield, W. J.: Effects of temperature and precipitation on snowpack variability in the Central Rocky Mountains as a function of elevation, Geophysical Research Letters, 42, 4429–4438, https://doi.org/10.1002/2015GL063898, 2015.

Speich, M. J., Bernhard, L., Teuling, A. J., and Zappa, M.: Application of bivariate mapping for hydrological classification and analysis of temporal change and scale effects in Switzerland, Journal of Hydrology, 523, 804–821, https://doi.org/10.1016/j.jhydrol.2015.01.086, 2015.

Staudinger, M., Weiler, M., and Seibert, J.: Quantifying sensitivity to droughts – an experimental modeling approach, Hydrology and Earth System Sciences, 19, 1371–1384, https://doi.org/10.5194/hess-19-1371-2015, 2015.

Switanek, M. B., Troch, P. A., Castro, C. L., Leuprecht, A., Chang, H.-I., Mukherjee, R., and Demaria, E. M. C.: Scaled distribution mapping: A bias correction method that preserves raw climate model projected changes, Hydrology and Earth System Sciences, 21, 2649–2666, https://doi.org/10.5194/hess-21-2649-2017, 2017.

Tedesche, M. E., Dahl, T. A., and Giovando, J. J.: Changing Snow Regime Classifications Across the Contiguous United States, Water Resources Research, 61, 470, https://doi.org/10.1029/2025WR041066, 2025.

Teutschbein, C., Grabs, T., Karlsen, R. H., Laudon, H., and Bishop, K.: Hydrological response to changing climate conditions: Spatial streamflow variability in the boreal region, Water Resources Research, 51, 9425–9446, https://doi.org/10.1002/2015WR017337, 2015.

Tropper, P. and Recheis, A.: Garnet zoning as a window into the metamorphic evolution of a crystalline complex: the northern and central Austroalpine Ötztal-Complex as a polymorphic example, Mitteilungen der Österreichischen Geologischen Gesellschaft, 94, 27–53, 2003.

Untersweg, T. and Schwendt, A.: Die Quellen der Blockgletscher in den Niederen Tauern.

Untersweg, T. and Schwendt, A.: Blockgletscher und Quellen in den Niedern Tauern, Mitteilungen der Österreichischen Geologischen Gesellschaft, 87, 47–55, 1996.

https://doi.org/10.5194/egusphere-2026-3664
Preprint. Discussion started: 22 July 2026

Valéry, A.: Modélisation précipitations – débit sous influence nivale Elaboration d'un module neige et évaluation sur 380 bassins versants, Dissertation, AgroParisTech, Paris, 2010.

Valéry, A., Andréassian, V., and Perrin, C.: 'As simple as possible but not simpler': What is useful in a temperature-based snow-accounting routine? Part 2 – Sensitivity analysis of the Cemaneige snow accounting routine on 380 catchments, Journal of Hydrology, 517, 1176–1187, https://doi.org/10.1016/j.jhydrol.2014.04.058, 2014a.

Valéry, A., Andréassian, V., and Perrin, C.: 'As simple as possible but not simpler': What is useful in a temperature-based snow-accounting routine? Part 1 – Comparison of six snow accounting routines on 380 catchments, Journal of Hydrology, 517, 1166–1175, https://doi.org/10.1016/j.jhydrol.2014.04.059, 2014b.

van Husen, D.: LGM and late-glacial fluctuations in the Eastern Alps, Quaternary International, 38/39, 109–118, 1997.

van Loon, A. F., Ploum, S. W., Parajka, J., Fleig, A. K., Garnier, E., Laaha, G., and van Lanen, H. A. J.: Hydrological drought types in cold climates: Quantitative analysis of causing factors and qualitative survey of impacts, Hydrology and Earth System Sciences, 19, 1993–2016, https://doi.org/10.5194/hess-19-1993-2015, 2015.

Viviroli, D., Dürr, H. H., Messerli, B., Meybeck, M., and Weingartner, R.: Mountains of the world, water towers for humanity: Typology, mapping, and global significance, Water Resources Research, 43, W07 447, https://doi.org/10.1029/2006WR005653, 2007.

Viviroli, D., Drenkhan, F., Scott, C. A., Somers, L., and van Tiel, M.: Cascading downstream impacts of water cycle changes in mountain regions, Nature Climate Change, 16, 129–142, https://doi.org/10.1038/s41558-025-02552-2, 2026.

Vremec, M., Seelig, M., Seelig, S., Collenteur, R., Haslinger, K., Wagner, T., Eybl, J., and Winkler, G.: Trend analysis of Alpine spring discharge: Interplay between climate and discharge characteristics, The Science of the total environment, 993, 179 875, https://doi.org/10.1016/j.scitotenv.2025.179875, 2025.

Wagner, T., Pauritsch, M., and Winkler, G.: Impact of relict rock glaciers on spring and stream flow of alpine watersheds: Examples of the Niedere Tauern Range, Eastern Alps (Austria), Austrian Journal of Earth Sciences, 109, 84–98, https://doi.org/10.17738/ajes.2016.0006, 2016.

Wagner, T., Brodacz, A., Krainer, K., and Winkler, G.: Active rock glaciers as shallow groundwater reservoirs, Austrian Alps, Grundwasser, 37, 215–230, https://doi.org/10.1007/s00767-020-00455-x, 2020a.

Wagner, T., Pleschberger, R., Kainz, S., Ribis, M., Kellerer-Pirklbauer, A., Krainer, K., Philippitsch, R., and Winkler, G.: The first consistent inventory of rock glaciers and their hydrological catchments of the Austrian Alps, Austrian Journal of Earth Sciences, 113, 1–23, https://doi.org/10.17738/ajes.2020.0001, 2020b.

Wagner, T., Ribis, M., Kellerer-Pirklbauer, A., Krainer, K., and Winkler, G.: The Austrian rock glacier inventory RGI_1 and the related rock glacier catchment inventory RGCI_1 in ArcGis (shapefile) format, https://doi.org/10.1594/PANGAEA.921629, 2020c.

Wagner, T., Seelig, S., Helfricht, K., Fischer, A., Avian, M., Krainer, K., and Winkler, G.: Assessment of liquid and solid water storage in rock glaciers versus glacier ice in the Austrian Alps, Science of The Total Environment, 800, 149 593, https://doi.org/10.1016/j.scitotenv.2021.149593, 2021a.

Wagner, T., Seelig, S., Krainer, K., and Winkler, G.: Storage–discharge characteristics of an active rock glacier catchment in the Innere Ölgrube, Austrian Alps, Hydrological Processes, 35, e14 210, https://doi.org/10.1002/hyp.14210, 2021b.

Wilcoxon, F.: Individual Comparisons by Ranking Methods, Biometrics Bulletin, 1, 80–83, https://doi.org/10.2307/3001968, 1945.

Winkler, G., Pauritsch, M., Wagner, T., and Kellerer-Pirklbauer, A.: Reliktische Blockgletscher als Grundwasserspeicher in alpinen Einzugsgebieten der Niederen Tauern, 2016a.

https://doi.org/10.5194/egusphere-2026-3664
Preprint. Discussion started: 22 July 2026

Winkler, G., Wagner, T., Pauritsch, M., Birk, S., Kellerer-Pirklbauer, A., Benischke, R., Leis, A., Morawetz, R., Schreilechner, M. G., and Hergarten, S.: Identification and assessment of groundwater flow and storage components of the relict Schöneben Rock Glacier, Niedere Tauern Range, Eastern Alps (Austria), Hydrogeology Journal, 24, 937–953, https://doi.org/10.1007/s10040-015-1348-9, 2016b.

Winkler, G., Wagner, T., Krainer, K., Ribis, M., and Hergarten, S.: Hydrogeology of Rock Glaciers - Storage Capacity and Drainage Dynamics - An Overview, in: Novel methods and results of landscape research in Europe, Central Asia and Siberia, edited by Sychev, V. G. and Mueller, L., pp. 329–334, FGBNU VNII agrochimii, Moskau, 2018.

Würzer, S., Jonas, T., Wever, N., and Lehning, M.: Influence of Initial Snowpack Properties on Runoff Formation during Rain-on-Snow Events, Journal of Hydrometeorology, 17, 1801–1815, https://doi.org/10.1175/JHM-D-15-0181.1, 2016.

Žebre, M., Colucci, R. R., Giorgi, F., Glasser, N. F., Racoviteanu, A. E., and Del Gobbo, C.: 200 years of equilibrium-line altitude variability across the European Alps (1901−2100), Climate Dynamics, 56, 1183–1201, https://doi.org/10.1007/s00382-020-05525-7, 2021.